Heliophysics Summer School 2026

Observational Heliophysics II: Photons from EUV to IR

Doug Rabin

ADVANCING THE SCIENCE OF
HELIOPHYSICS

A partnership between NASA UCAR COMMUNITY PROGRAMS | CPAESS

Thanks to

Lika Guhathakurta

Farzad Kamalabadi

Nick Gross

UCAR

and

Thanks to all of you for your participation!

Goals

- Discuss two key topics in enough depth to give you an entry point into the physics and the state of the art.
- Focus on magnetic fields and temperature distribution because of their central importance in solar physics and heliophysics more broadly.
- Many important topics can’t be covered!

What’s missing?

- Paschen-Back effect (strong magnetic fields)
- Stark effect (electric fields)
- Zeeman and Hanle effects in molecules
- Stokes inversion techniques
- X rays, gamma rays (for radio waves, tune in tomorrow)
- Methods for measuring particle number density and elemental abundances
- Helioseismology
- Heliospheric imaging
- Radiance and irradiance (spectral and total)
- Feature tracking
- … and more

But too beautiful to miss entirely ...

NASA Scientific Visualization Studio
https://svs.gsfc.nasa.gov/31375/

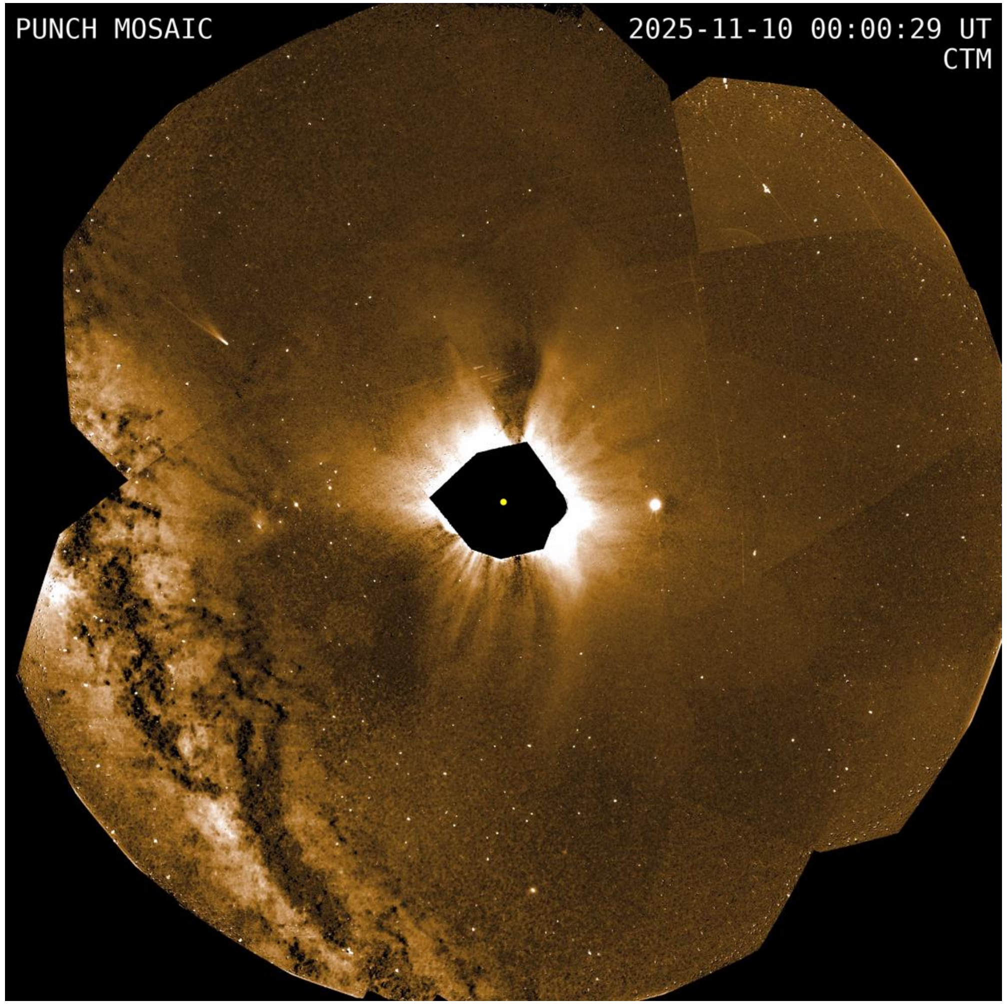

Courtesy of Craig DeForest and the PUNCH Team

Life is a spectrum

https://www.spaceweather.gov/content/aurora-tutorial

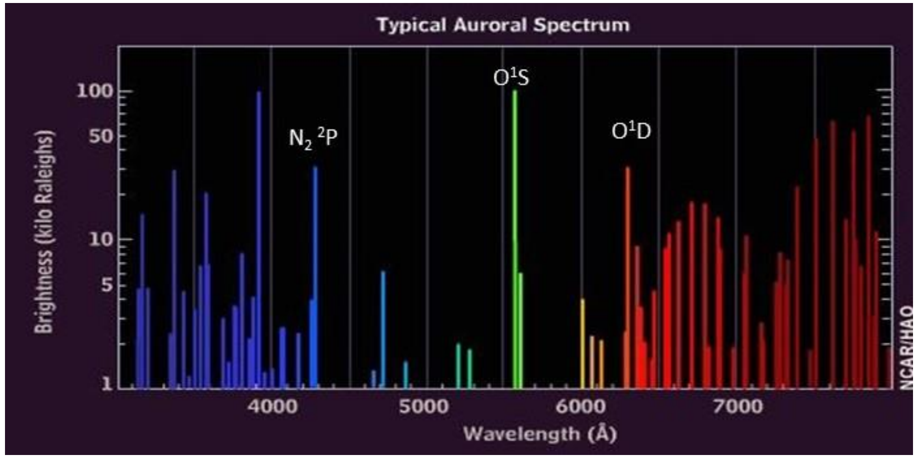

Table 1. List of atomic transitions taken into account in the simulations.

Species	Transition	Wavelength (nm)	References	Width (nm)	Comments
O I	$^1S \rightarrow {}^1D$	557.7	(Kramida et al., 2022)	0.2	Forbidden transition; lifetime ∼ 1 s.
O I	$^1D \rightarrow {}^3P$	630 and 636 and 639	(Kramida et al., 2022)	0.2	Forbidden triplet transition; lifetime ∼110 s.
O I	$3p^5P \rightarrow 3s^5\ S^0$	777.2 and 777.4 and 777.5	(Kramida et al., 2022)	0.2	Triplet transitions.
O I	$3p^3\ P \rightarrow 3s^3\ S^0$	844.6	(Kramida et al., 2022)	0.2	Triplet transitions but with very close lines. We consider this line as a single line.
O II	$^2P \rightarrow {}^2D$	732.0	(Kramida et al., 2022)	0.2	
N I	$^2D \rightarrow {}^4S$	520	(Kramida et al., 2022)	0.2	Forbidden transition; lifetime ∼9.95 h.
N II	$3d^3\ F \rightarrow 3p^3\ D$	500.1 and 500.5	(Kramida et al., 2022)	0.2	
N II	$3p^3\ D \rightarrow 3s^3\ P$	568.0	(Kramida et al., 2022)	0.2	In fact four different lines. Only the 568.0 nm has a significant cross-section. The other three have been included in the other lines (see below).
N I and N II	81 lines listed in Table 18 of Mangina et al. (2011)	From 380 to 900	(Mangina et al., 2011)	0.2	The weak lines of the two previous multiplets have been included in these 81 lines.

?

Species	Transition
O I	$^1S \rightarrow {}^1D$
O I	$^1D \rightarrow {}^3P$
O I	$3p^5P \rightarrow 3s^5\ S^0$
O I	$3p^3\ P \rightarrow 3s^3\ S^0$
O II	$^2P \rightarrow {}^2D$
N I	$^2D \rightarrow {}^4S$
N II	$3d^3\ F \rightarrow 3p^3\ D$
N II	$3p^3\ D \rightarrow 3s^3\ P$

Mathieu+, SWSC, 15 (2025), doi:10.1051/swsc/2025013

Outline

- What do we want to measure?
- Quick refresher on spectroscopic nomenclature
- Polarization and Stokes parameters
- Zeeman effect
- Hanle and magneto-optical effects
- Stokes analysis
- Differential emission measure (temperature distribution)

What do we want to measure?

- Temperature
- Density
- Composition
- Ionization states
- Bulk velocity vector and turbulent velocities
- Magnetic and electric field vectors
- Radiances

➡ All these quantities may vary in space and time and are subject to line-of-sight confusion and other optical depth effects.

LS coupling of angular momentum

LS (Russell-Saunders) Coupling

- In light atoms (typically Z≤30), electron spins interact among themselves to form a total spin angular momentum ***L***.
- The same happens with orbital angular momentum to form total orbital angular momentum ***S***.
- ***S*** and ***L*** couple to form total angular momentum ***J***.
- The quantum number J can assume integer values in the range $|L - S| \le J \le |L + S|$, giving $2S + 1$ possible values when $L > S$.

jj Coupling

- In heavier atoms, the spin-orbit interaction may be comparable or larger than spin-spin or orbit-orbit interactions.
- In the limiting case, the individual spin and orbital angular momenta combine to form a total angular momentum for each electron, $\boldsymbol{j_i}$.
- The $\boldsymbol{j_i}$ sum to form ***J***.
- LS coupling is far more common in solar applications. We won't further consider jj coupling.

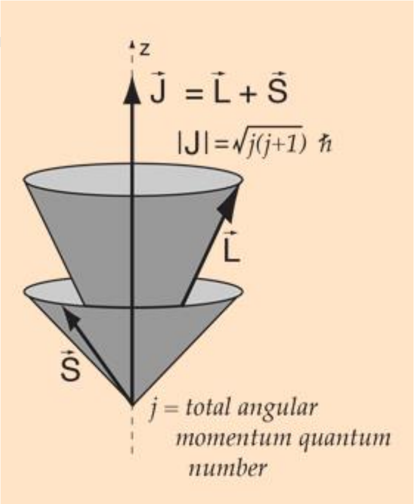

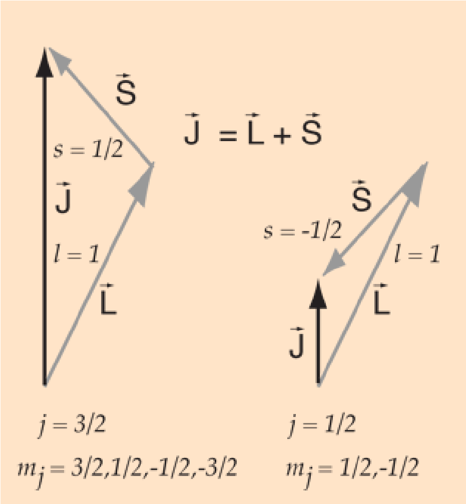

http://www.hyperphysics.phy-astr.gsu.edu/hbase/Atomic/lcoup.html

Spectroscopic Nomenclature in LS Coupling

$$^{2S+1}L_J^o$$

Specify	Name
S, L	term (multiplet)
S, L, J	level (line)
S, L, J, m_J	state (line component)

- 2S+1 is the spin multiplicity. For example, S = 1 yields a triplet.
  - If S > L, the multiplicity is 2L+1, but 2S+1 is still used in the term symbol.
- For historical reasons, L = 0,1,2,3 is written S, P, D, F.
- Superscript o designates odd parity, $P = (-1)^{\sum_i l_i}$. Omitted when parity is even.

Specifying a spectral line transition

- Example: Fe I 617.33 nm (used by the Helioseismic and Magnetic Imager on SDO)

term resulting from coupling within $3d^7$ group

number of equivalent electrons in d subshell

principal quantum number

orbital angular momentum (l=2) of each electron in subshell

$$3d^7(^4F)4p\ ^5P_1 - 3d^7(^4D)4s\ ^5D_0^o$$

upper level

lower level

- Completely filled shells corresponding to a noble gas are conventionally omitted from the written configuration. In this example, in a full description, $3d^7$ would be preceded by $1s^2 2s^2 2p^6 3s^2 3p^6$, the configuration of neutral argon.

Where to find data on atomic spectra

https://www.chiantidatabase.org/

CHIANTI

An Atomic Database for Spectroscopic Diagnostics of Astrophysical Plasmas

Version 11.0.4 of the CHIANTI IDL routines released, June 2026

https://www.nist.gov/pml/atomic-spectra-database

Atomic Spectra Database

NIST Standard Reference Database 78

Version 5.12

Last Update to Data Content: November 2024 | Version History & Citation Information | Disclaimer | DOI: https://dx.doi.org/10.18434/T4W30F

Welcome to the NIST Atomic Spectra Database, NIST Standard Reference Database #78. The spectroscopic data may be selected and displayed according to wavelengths or energy levels by choosing one of the following options:

LINES	Spectral lines and associated energy levels displayed in wavelength order with all selected spectra intermixed or in multiplet order. Transition probabilities for the lines are also displayed where available.
LEVELS	Energy levels of a particular atom or ion displayed in order of energy above the ground state.
GROUND STATES & IONIZATION ENERGIES	Ground states and ionization energies of atoms and atomic ions.
LIBS	ASD Interface for Laser Induced Breakdown Spectroscopy (LIBS)

Polarization

A monochromatic ray propagating in the z direction can be described by two independent orthogonal components of the electric field vector (in phasor form) with a time-invariant phase relationship:

$$\vec{E}(z,t) = \hat{x}\, E_{0x} e^{i(kz-\omega t+\delta_x)} + \hat{y}\, E_{0y} e^{i(kz-\omega t+\delta_y)} = \underbrace{\left[\hat{x}\, E_{0x} e^{i\delta_x} + \hat{y}\, E_{0y} e^{i\delta_y}\right]}_{\text{Jones vector}} \underbrace{e^{i(kz-\omega t)}}_{\text{propagator}}$$

Convert this to real form and eliminate the propagator between the equations to yield a *polarization ellipse*:

$$\frac{E_x(z,t)^2}{E_{0x}^2} + \frac{E_y(z,t)^2}{E_{0y}^2} - \frac{2E_x(z,t)E_y(z,t)}{E_{0x}E_{0y}} \cos\delta = \sin^2\delta \quad \text{where } \delta = \delta_y - \delta_x$$

At constant z, the tip of the electric vector traces an ellipse as time progresses. The properties of the ellipse can be related to E_{0x}, E_{0y}, and δ — we don't need the equations here. The progression can be clockwise or counterclockwise (chirality).

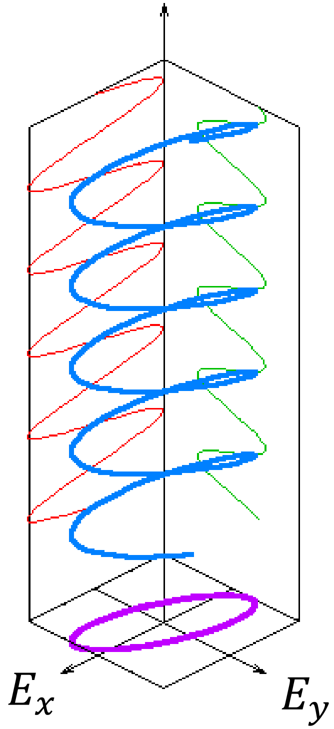

While true, this simple picture is not enough for remote observers of the Sun:

1. Sunlight is not completely polarized.
2. We need to relate the state of polarization to observable radiances, not $\vec{E}$.

This leads us to the *Stokes vector*.

Stokes vector

Wikipedia

George Stokes
(1819 – 1903)

In terms of the electric field, the Stokes vector $\{I, Q, U, V\}$ is defined as*

$$I = \langle E_x^2 + E_y^2 \rangle \quad Q = \langle E_x^2 - E_y^2 \rangle \quad U = \langle 2E_x E_y \cos\delta \rangle \quad V = \langle 2E_x E_y \sin\delta \rangle$$

where the brackets signify time averages. Note that the vector can also be expressed using an orthogonal basis other than $(\hat{x}, \hat{y})$ — for example, linearly polarized components rotated 45° in the xy plane, or right and left circularly polarized components, $(\hat{x} \pm i\,\hat{y})/\sqrt{2}$.

Shurcliff[1] prefers to define the Stokes parameters operationally using measurements of irradiance. That's after all what we do in practice. We need at least four measurements; there are many possibilities. Here's a simple one using a linear polarizer (LP) and a quarter-wave plate (QWP).

Place in beam just before detector	Measured irradiance gives
1. LP oriented at 0°	$(I+Q)/2$
2. LP oriented at 45°	$(I+U)/2$
3. LP oriented at 90°	$(I-Q)/2$
4. QWP oriented at -45° followed by LP at 0°	$(I+V)/2$

$I^2 = Q^2 + U^2 + V$ completely polarized

$I^2 > Q^2 + U^2 + V$ partially polarized

Modern Stokes polarimeters use more elaborate schemes for sensitivity, efficiency and redundancy, but the idea is the same.

*The labels $\{S_0, S_1, S_2, S_3\}$ are often used instead of $\{I, Q, U, V\}$.

[1]Shurcliff, William A. *Polarized Light: Production and Use*, Cambridge, MA and London, England: Harvard University Press, 1962, doi/10.4159/harvard.9780674424135

Poincaré sphere*

A very handy tool for a magnetograph designer or aficionado because the action of a phase retarder (waveplate) corresponds to a rotation of the sphere about the fast axis of the waveplate. For example, if the fast axis is along $S_2 \equiv Q$, a quarter-wave plate will convert right circular polarization S_3 to linear polarization S_1 .

Wikipedia

Henri Poincaré
(1854 – 1912)

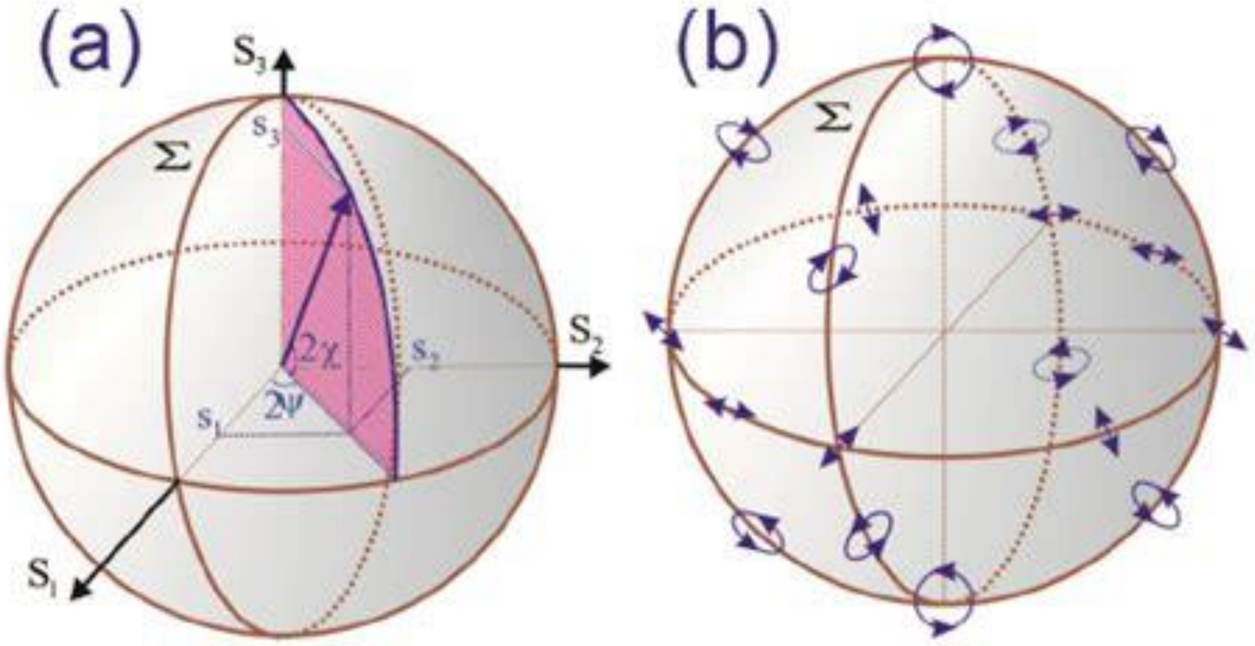

$$I = \text{radius of sphere}$$
$$Q = \cos 2\chi \cos 2\psi$$
$$U = \cos 2\chi \sin 2\psi$$
$$V = \sin 2\chi$$

Try a Poincaré sphere calculator and visualizer such as https://viveksabarad0221.github.io/poincare-bench/

- This site labels the Stokes axes H, V, D, A, R, L for horizontal, vertical, diagonal, and antidiagonal linear polarization, left and right circular polarization.

* It's a ball, but who's quibbling?

Zeeman effect

In an externally applied magnetic field, an atom acquires a magnetic potential energy $\Delta H = -\vec{\mu} \cdot \vec{B}$ where $\vec{\mu} = \mu_B(\vec{L} + 2\vec{S})/\hbar$ and μ_B is the Bohr magneton. In LS coupling, the change in energy of an atomic level is

$$V_m = \mu_B \, B \, m_j \, g_J \quad \text{where } \mu_B = {}^{e\hbar}/_{2m_e} \text{ and}$$

$$g_J = 1 + \frac{J(J+1) + S(S+1) - L(L+1)}{2J(J+1)} \quad \text{is the Landé g-factor}$$

The next slide illustrates the Zeeman splitting of energy levels. To connect that to the behavior of spectral lines, we remind ourselves of the selection rules for the strongest radiative transitions, electric dipole transitions:

electric dipole transition rules

$\Delta S = 0$

$\Delta L = 0, \pm 1$

$\Delta J = 0, \pm 1$ but $J = 0 \rightarrow J = 0$ is forbidden

$\Delta m_j = 0, \pm 1$ but $m_j = 0 \rightarrow m_j = 0$ is forbidden if $\Delta J = 0$

Wikipedia

Pieter Zeeman (1865 – 1943)
Shared with Hendrik Lorentz the 1902 Nobel Prize in Physics for "their researches into the influence of magnetism upon radiation phenomena"

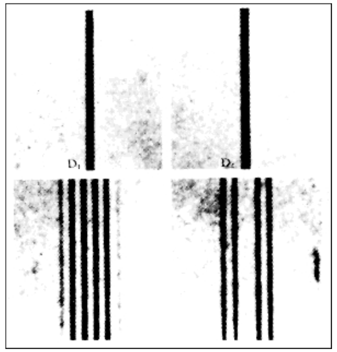

A photograph taken by Zeeman of the splitting of the Na D lines

Taste the forbidden

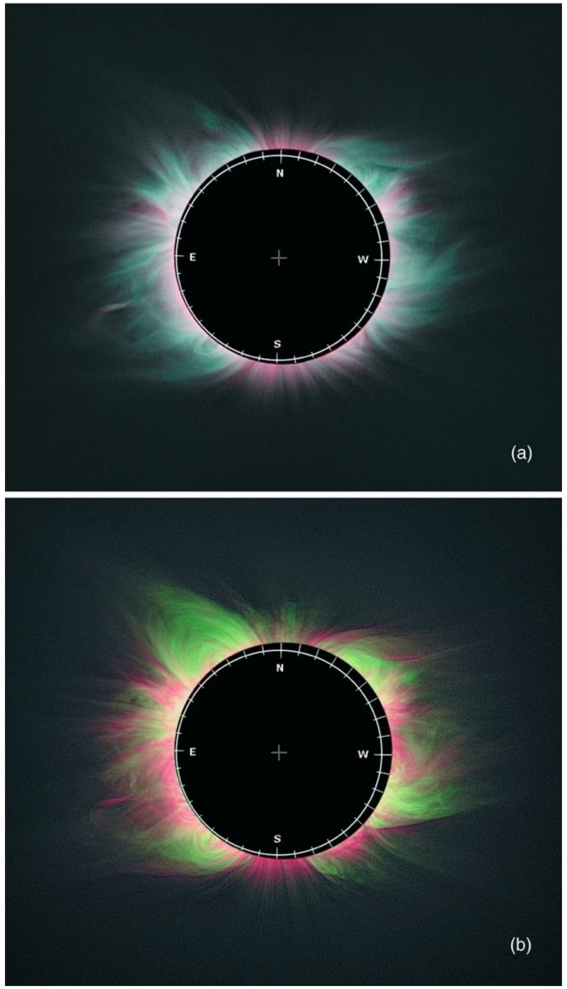

Figure 8. (a) Overlay of Fe X (red) and Fe XI (cyan). The same intensity in both lines produces a neutral gray. Red indicates a dominant Fe X emission while cyan indicates the dominance of Fe XI. (b) Overlay of Fe X (red) and Fe XIV (green). The same amount of these colors is yellow; red is when Fe X dominates and green is when Fe XIV dominates.

Habbal+, ApJ, 734 (2011), doi:10.1088/0004-637X/734/2/120

Zeeman components

Triplet (S = 0)

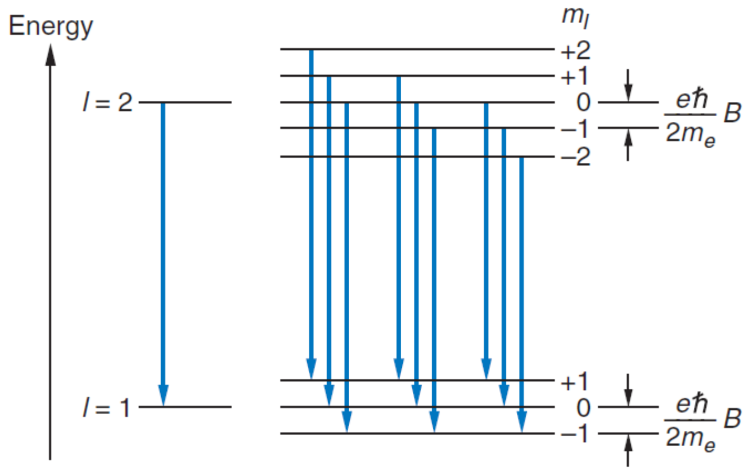

Energy-level splitting in a magnetic field for singlet (S=0) levels L=2 and L=1. Each level is split into (2L+1) terms. The 9 transitions consistent with Δm=0,±1 yield only 3 different energies because the energy difference between adjacent terms is independent of L.

Line components are labelled

π if Δm = 0

σ if Δm = ±1

The polarization of a component depends on our viewing direction relative to the direction of the magnetic field:

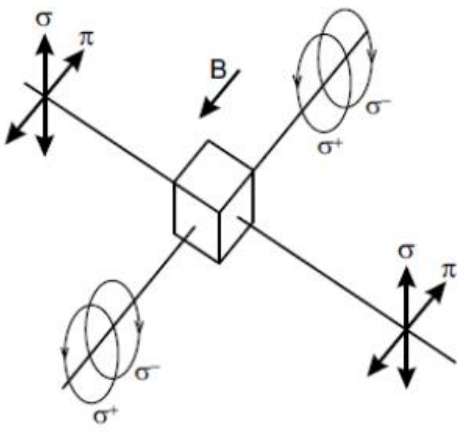

More complex patterns (S = 1)

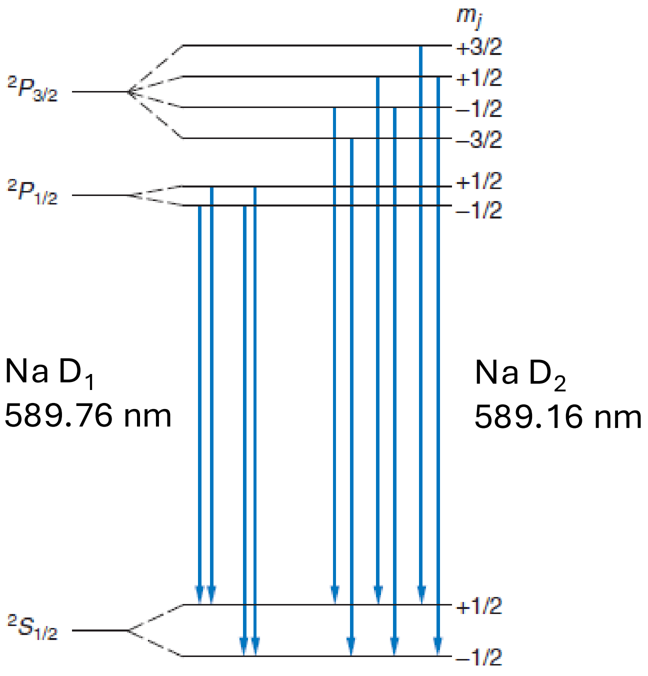

Energy-level splitting of 3 energy levels of the Na D lines in a magnetic field. The splitting depends on L, S, and J, resulting in 4 or 6 Zeeman components.

Stokes profiles in a magnetic field (highly simplified)

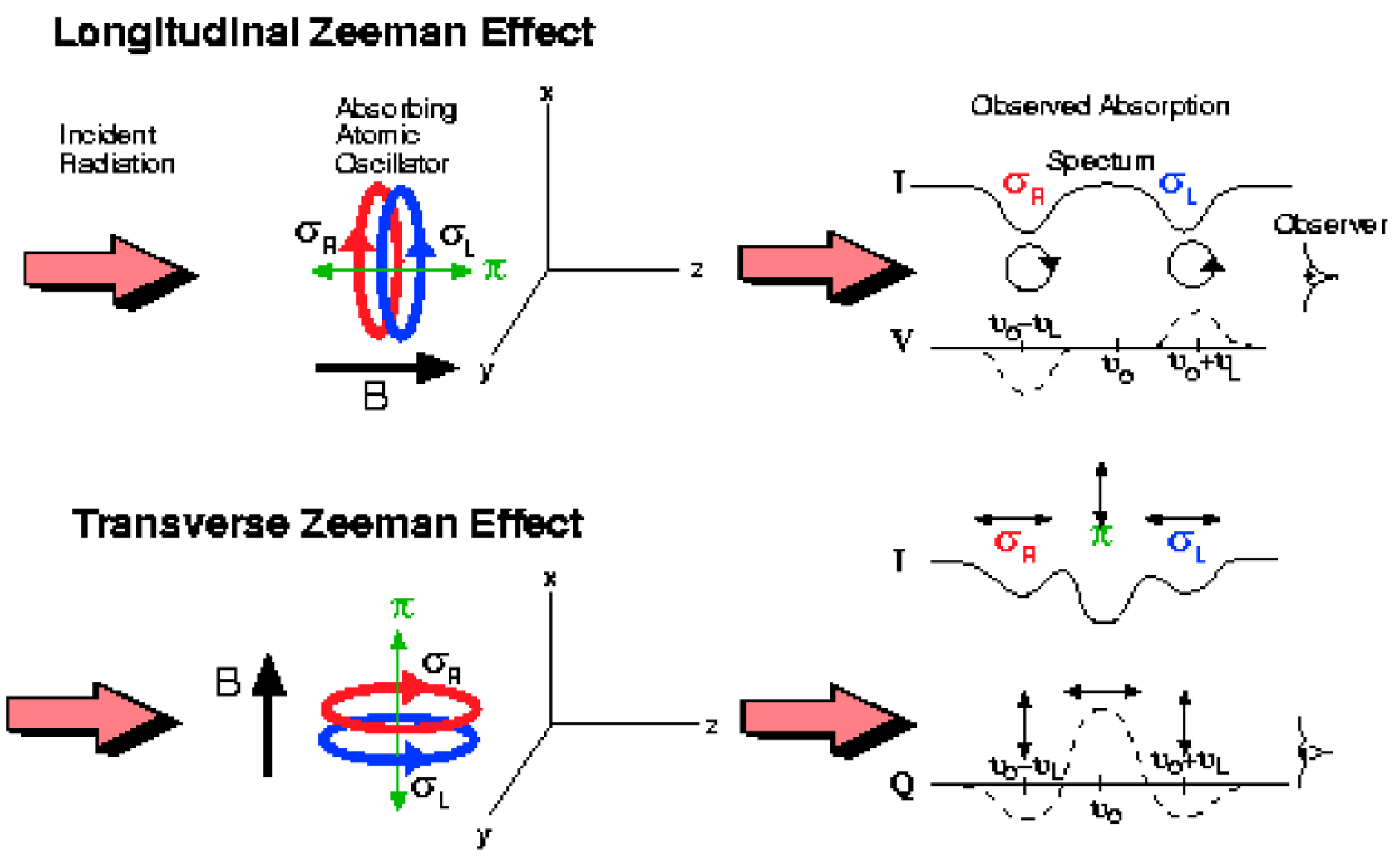

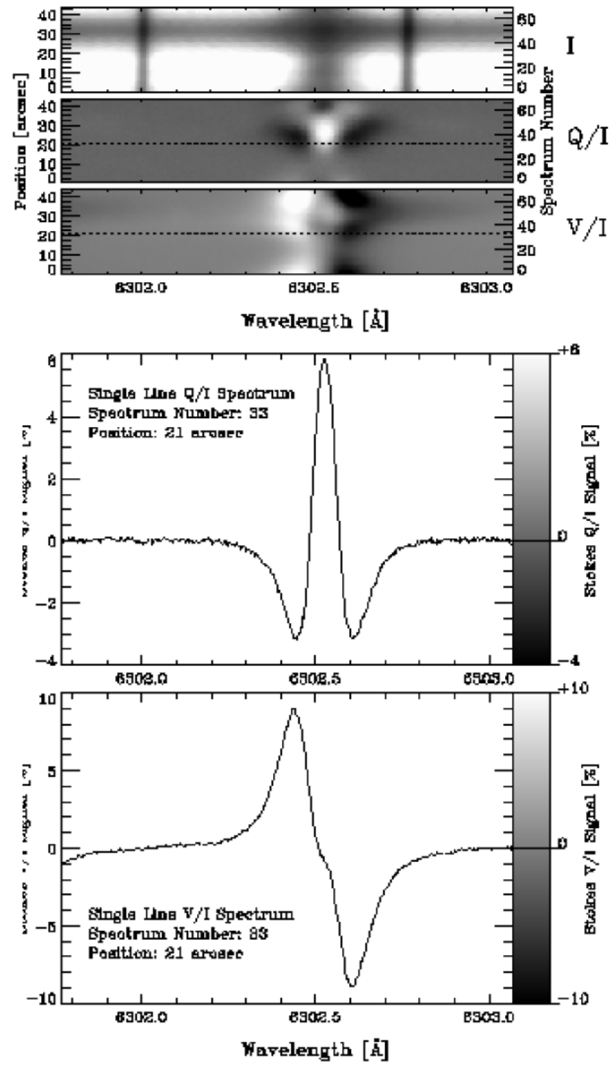

Slide credit: A. Gandorfer

Stokes profiles in a magnetic field

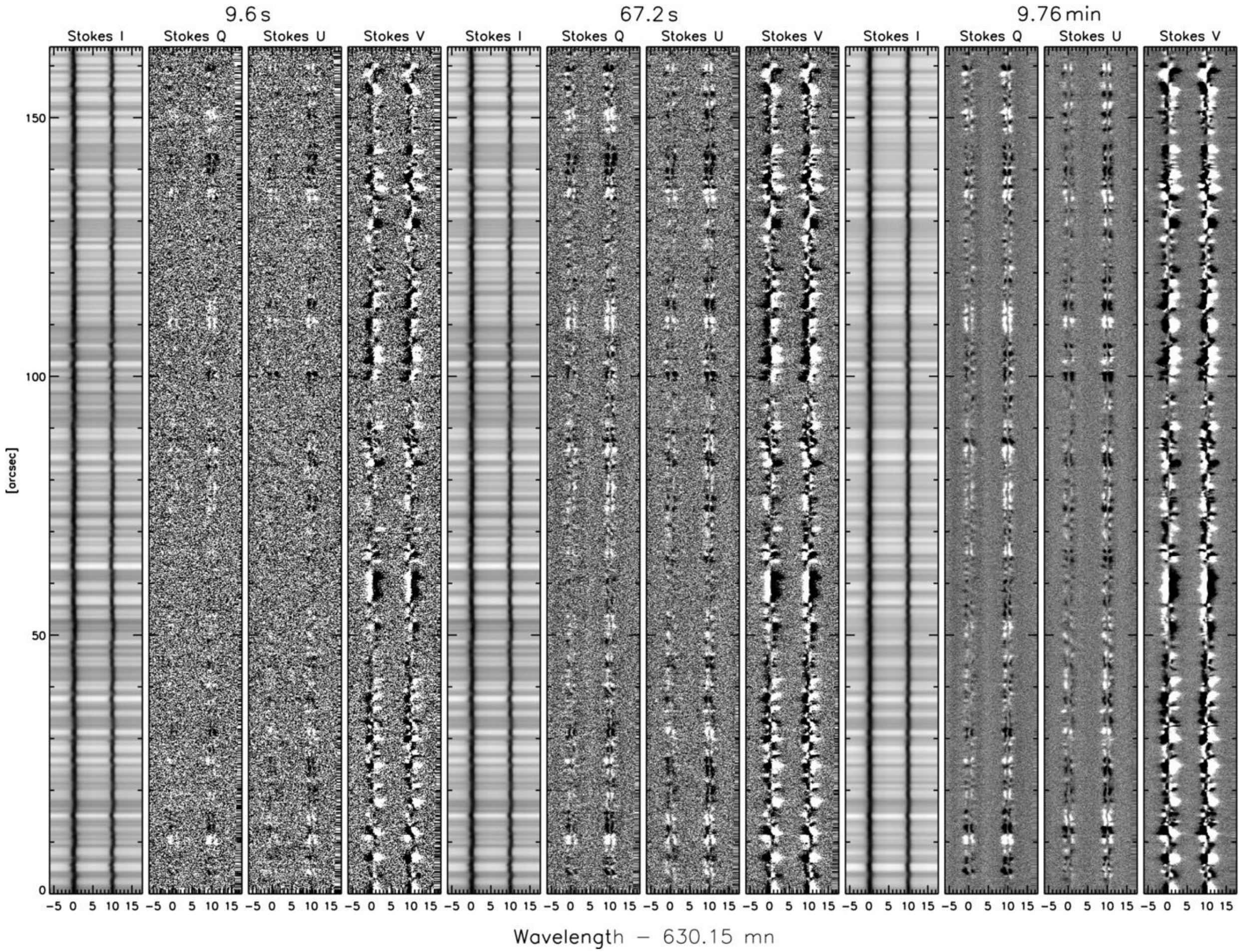

Spectra from Hinode SP of quiet Sun, disk center.
The contrast scale saturates at $\pm 10^{-3}\ I_{QS}$.

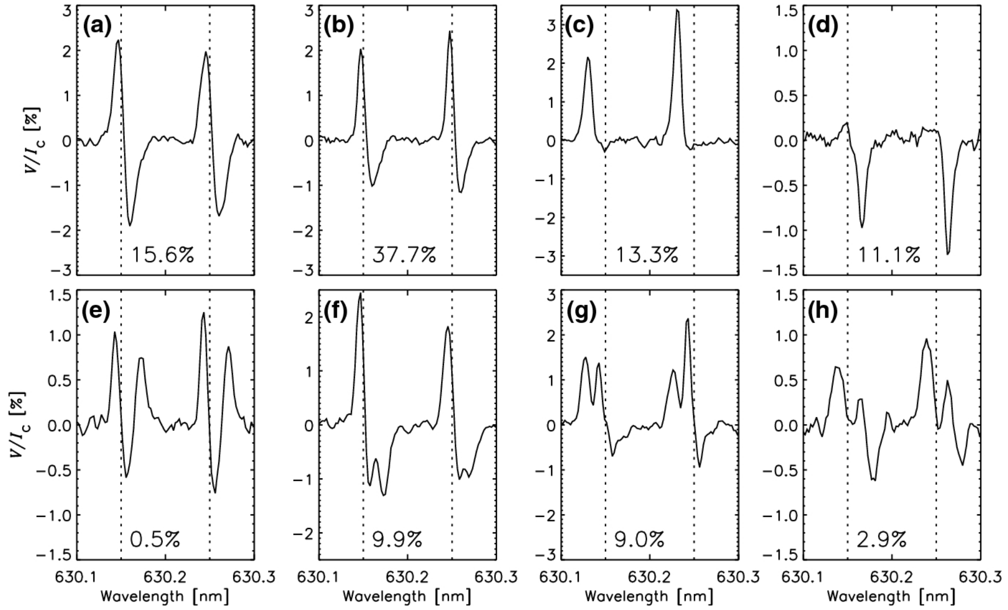

Classification of Fe I 630.15 and 630.25 nm Stokes *V* profiles observed by Hinode in a quiet Sun IN region at disk center with a resolution of 0.3 arcsec. The dotted lines indicate the central wavelengths of the two lines. The profiles exhibit distinct spectral signatures. Panel **a** displays a prototypical regular profile with two lobes of opposite sign. The other panels show profiles with increasingly larger asymmetries (**b**), only one lobe (**c** and **d**), three lobes (**e**), bumps in the one of the lobes (**f** and **g**), and even four lobes (**h**). The cause of these spectral features can be traced back to the physical processes at work on the solar surface. The numbers shown in each panel give the fraction of IN profiles belonging to the different classes, considering only those pixels with signals above 6 times the noise level

Bellot Rubio+, ApJ, 757 (2023),
doi:10.1088/0004-637X/757/1/19

Hanle Effect

Wikipedia

Wilhelm Hanle
(1901 – 1993)

Take-aways

- The Hanle effect in the Sun refers to the modification of scattering polarization by a local magnetic field.
- Scattering polarization is linear polarization caused by coherent scattering of anisotropic incident radiation. Scattering polarization has been measured in many solar spectral lines from the IR to EUV.
- The Hanle effect does not depend on the length of the path traveled in the magnetic field by the incident photon*, nor on its direction of incidence.
- The Hanle effect primarily operates near the center of a spectral line.
- The Hanle effect is a powerful tool for investigating magnetic fields in the rough range 1–100 G.

* This contrasts with the Faraday effect, which causes rotation of the plane of polarization proportional to the distance the atom has traveled through the magnetic medium.

Hanle Effect

Classical interpretation

- Hanle's interpretation was based on the Lorentz oscillator model, which treats an electron as bound to the nucleus by "springs", forming a damped harmonic oscillator.
- Linearly polarized incident light drives the electron to oscillate along the plane of polarization, forming an oscillating electric dipole with a finite lifetime.
- In an external magnetic field, the oscillating dipole precesses around the B-direction at the Larmor frequency.
- As the dipole rotates, the emitted radiation is distributed over a broader range of angles than the non-rotating dipole. Averaged over the radiative lifetime, the net polarization is reduced, and the polarization pattern is modified.

Quantum interpretation

- For a certain range of field strength, the Zeeman sublevels are close enough in energy that the natural line widths of the sublevels overlap significantly (phase coherence).
- When the sublevels are separated by significantly more than a natural line width, coherence is lost, the degree of polarization of the scattered radiation is independent of field strength, and the effect is said to be *saturated*. The saturated Hanle effect cannot measure magnetic field strength but remains sensitive to the direction of the field.

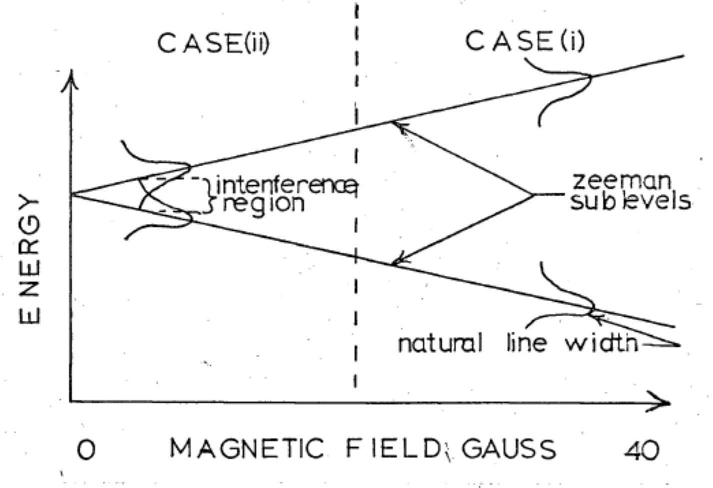

R. Bardsley, UBC Thesis 1970

Magneto-optical Effect

Art by J. Scott Campbell

Magneto
(1963 –)

- In a nutshell: An optically active medium in the presence of a magnetic field can change the polarization of light as it passes through the medium.
- Faraday effect (induced circular birefringence)
  - Medium acts as a circular retarder because it has a different refractive index for right circularly polarized (RCP) and left circularly polarized (LCP) rays.
  - If an incident linearly polarized (LP) ray is decomposed into RCP and LCP rays, the medium introduces a cumulative phase shift between the components as they traverse the medium.
  - The exit ray is LP but has a different direction than the incident ray.
- Voigt effect (induced linear birefringence)
  - Description as above with the roles of CP and LP reversed. The medium acts as a linear retarder.
  - The exit ray is elliptically polarized along a different axis than the direction of the incident LP ray.

- Magneto-optical effects are most often observed in the wings of a spectral line but can also produce small polarization effects at line center.

Where to find the gory details

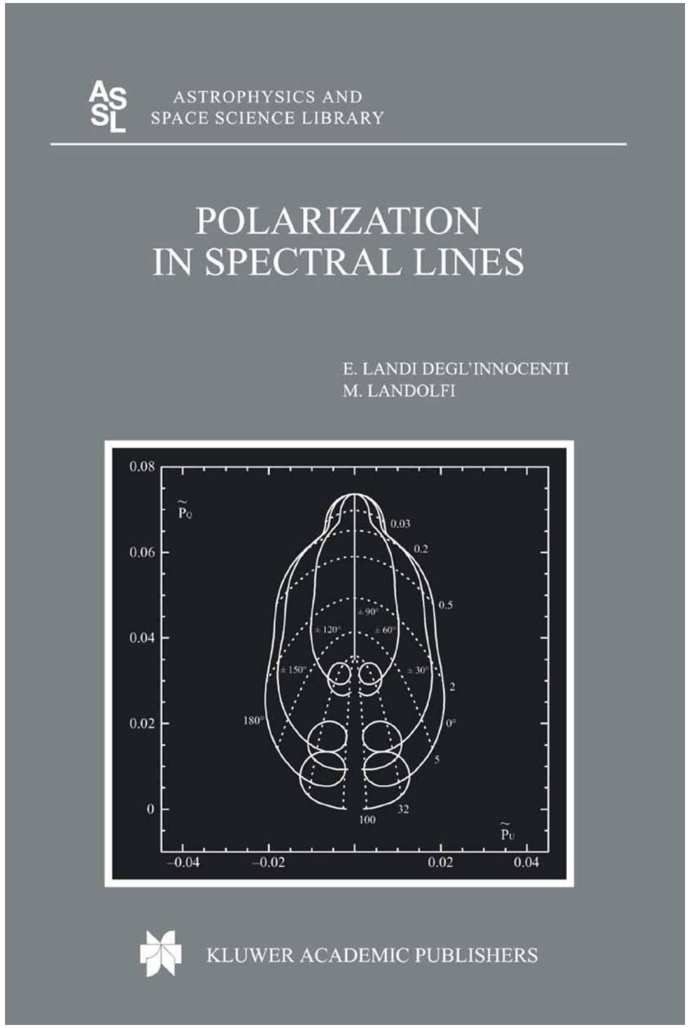

Polarization in Spectral Lines. Egidio Landi Degl'Innocenti and Marco Landolfi, University of Firenze, Firenze, Italy; Arcetri Observatory, Firenze, Italy. 2004, Astrophysics and Space Library, Volume 307, Kluwer Academic Publishers, Dordrecht

doi:10.1007/978-1-4020-2415-3

The Stokes zoo

- "An atlas of theoretical Stokes profiles for solar disk observations"* displays the wide variety of Stokes patterns that arise even from a simplified model of line formation in a magnetic field.
- Assumptions
  - One-dimensional, plane-parallel atmosphere with constant magnetic field
  - Source function varies linearly with optical depth (Milne-Eddington)
  - Constant ratio between line and continuous absorption coefficients
  - Normal Zeeman triplet with Gaussian profiles
  - No bulk velocities
- The models are characterized by
  - $\eta_0 =$ line absorption coefficient / continuous absorption coefficient
    - Models are shown for η_0 = 1 (weak line) and η_0 = 7 (strong line)
  - $v_H =$ Zeeman splitting / Doppler width
    - Models are shown for v_H = 0.1 (weak splitting) and v_H = 2.5 (strong splitting)
  - ψ is the inclination of $\vec{B}$ to the line of sight.
  - ϕ is the azimuth angle of $\vec{B}$ in the plane perpendicular to the LOS.

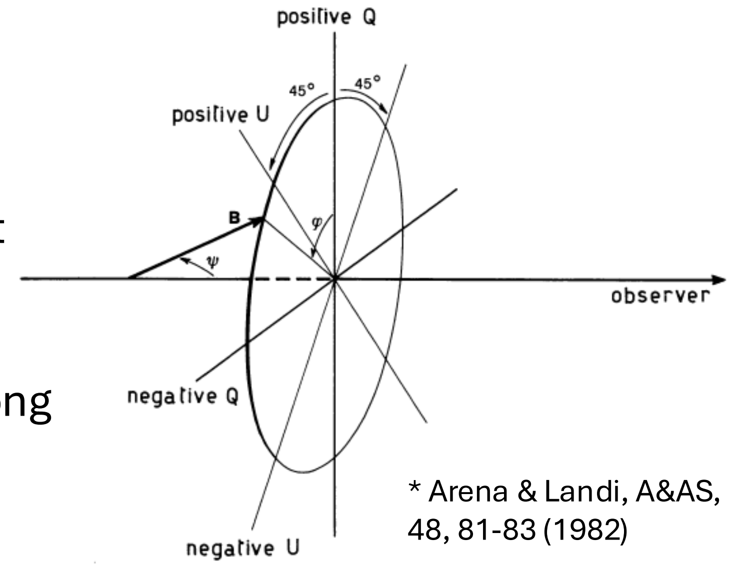

* Arena & Landi, A&AS, 48, 81-83 (1982)

The Stokes zoo

Weak line (η_0 = 1) and weak splitting (v_H = 0.1)

Nearly longitudinal $\vec{B}$ Nearly transverse $\vec{B}$

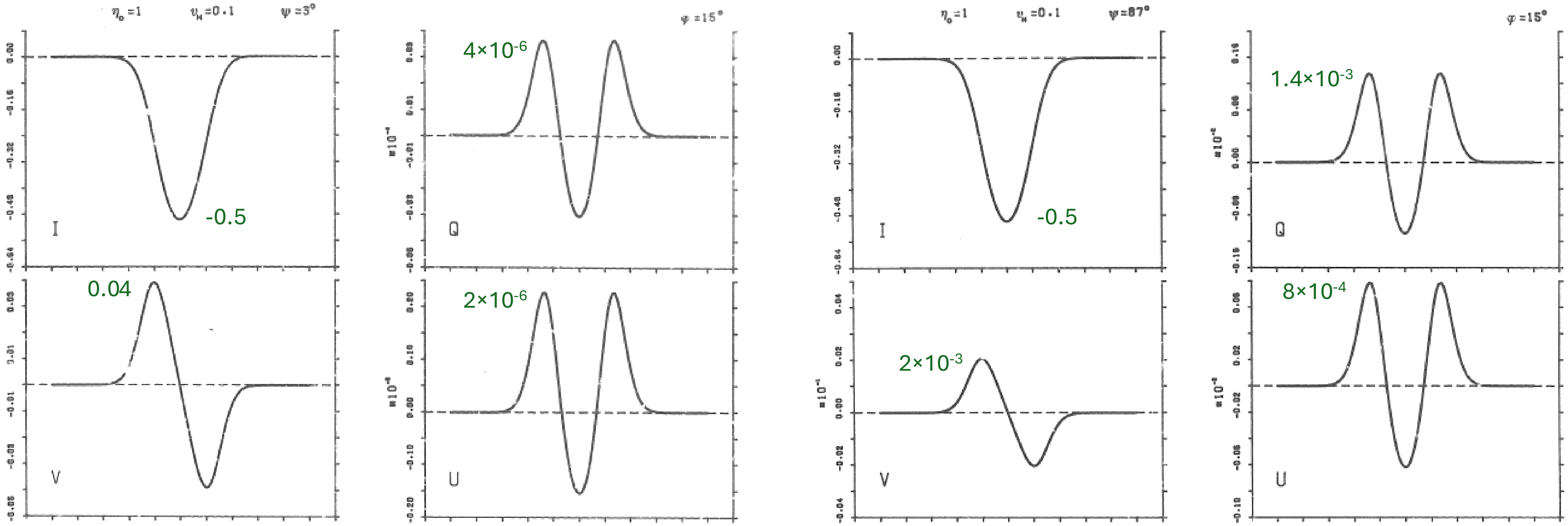

➡ It is not necessary to plot all values of ψ and ϕ because of the following relationships:

$Q(\phi + \alpha) = \cos 2\alpha\, Q(\phi) - \sin 2\alpha\, Q(\phi)$ $U(\phi + \alpha) = \sin 2\alpha\, Q(\phi) + \cos 2\alpha\, U(\phi)$

$I(180° - \psi, - \phi) = I(\psi, \phi)$ $Q(180° - \psi, - \phi) = Q(\psi, \phi)$ $U(180° - \psi, - \phi) = -U(\psi, \phi)$ $V(180° - \psi, - \phi) = -V(\psi, \phi)$

The Stokes zoo

Weak line (η_0 = 1) and strong splitting (v_H = 2.5)

Nearly longitudinal $\vec{B}$

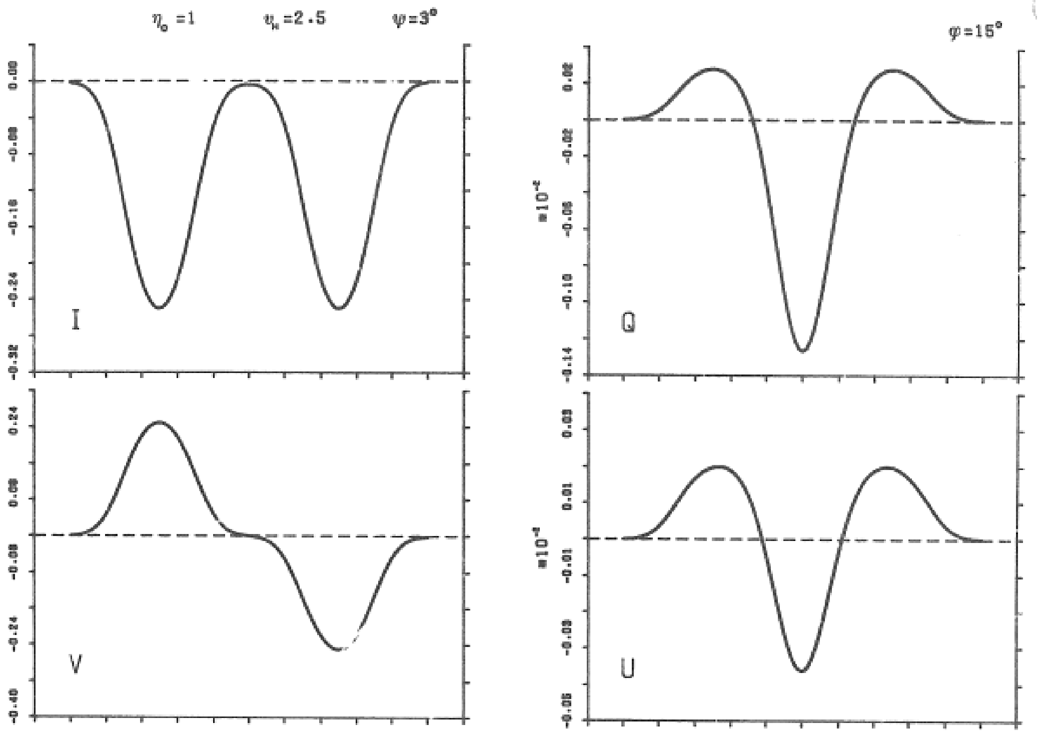

Nearly transverse $\vec{B}$

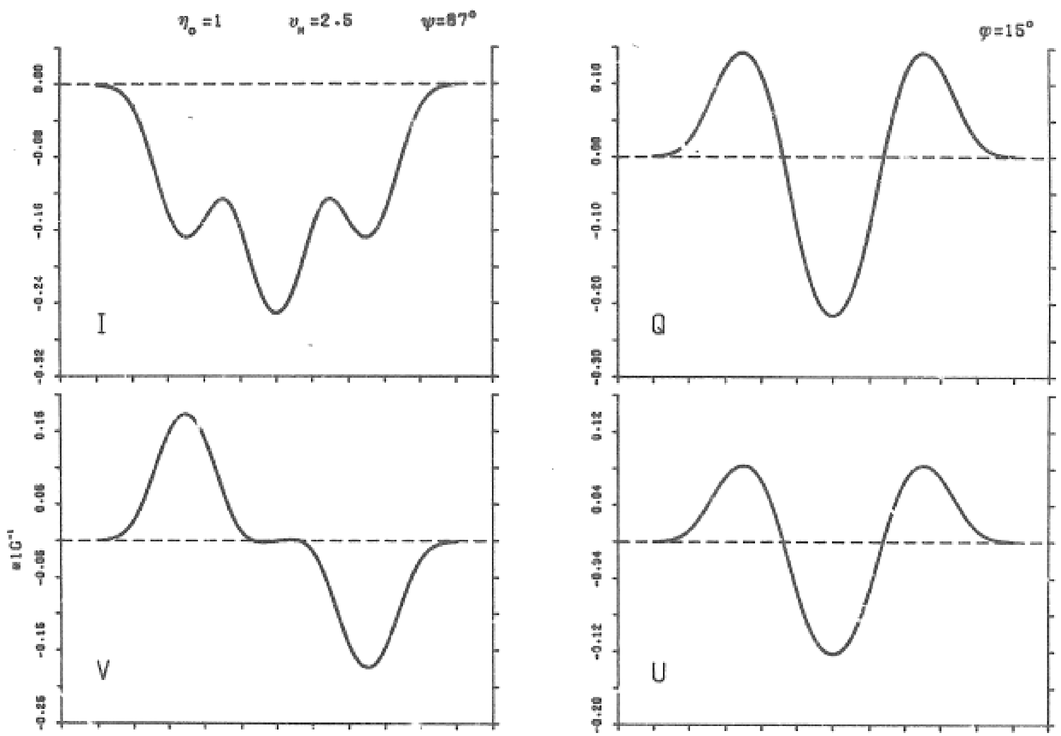

The Stokes zoo

Strong line (η_0 = 7) and weak splitting (v_H = 0.1)

Nearly longitudinal $\vec{B}$

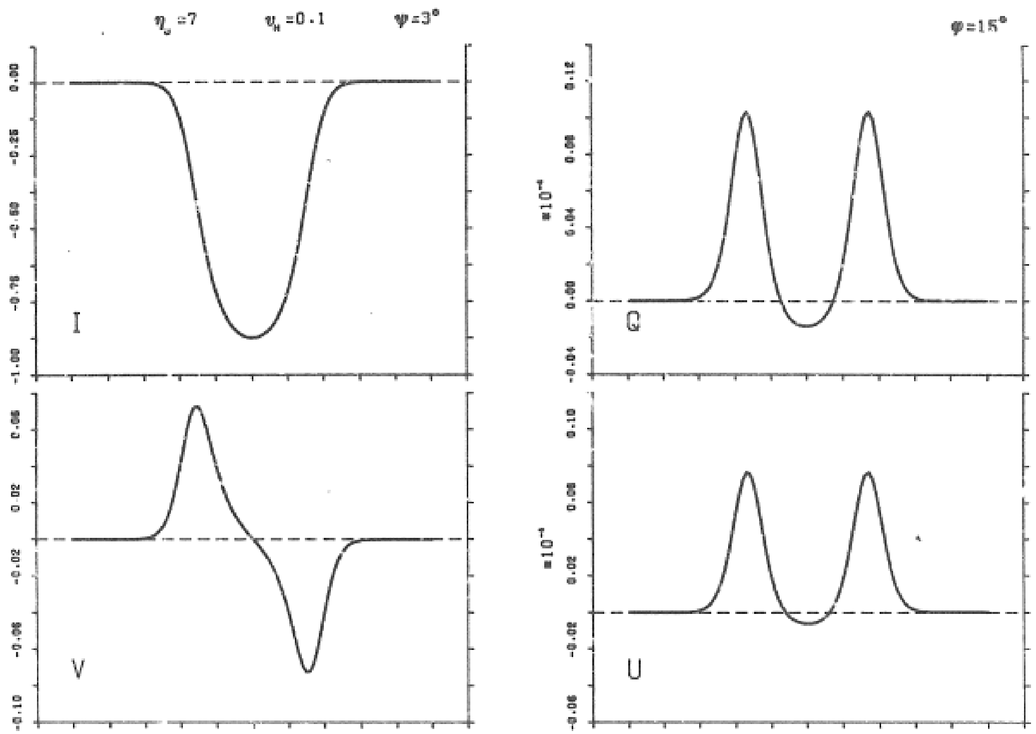

Nearly transverse $\vec{B}$

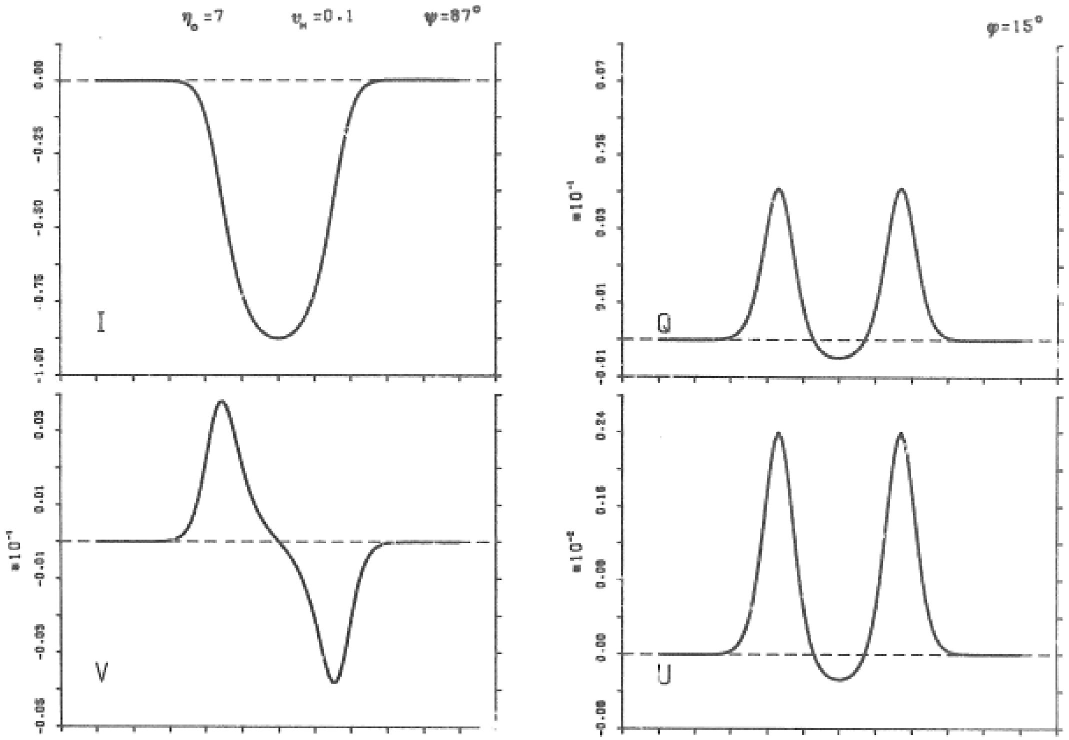

The Stokes zoo

Strong line (η_0 = 7) and strong splitting (υ_H = 2.5)

Nearly longitudinal $\vec{B}$

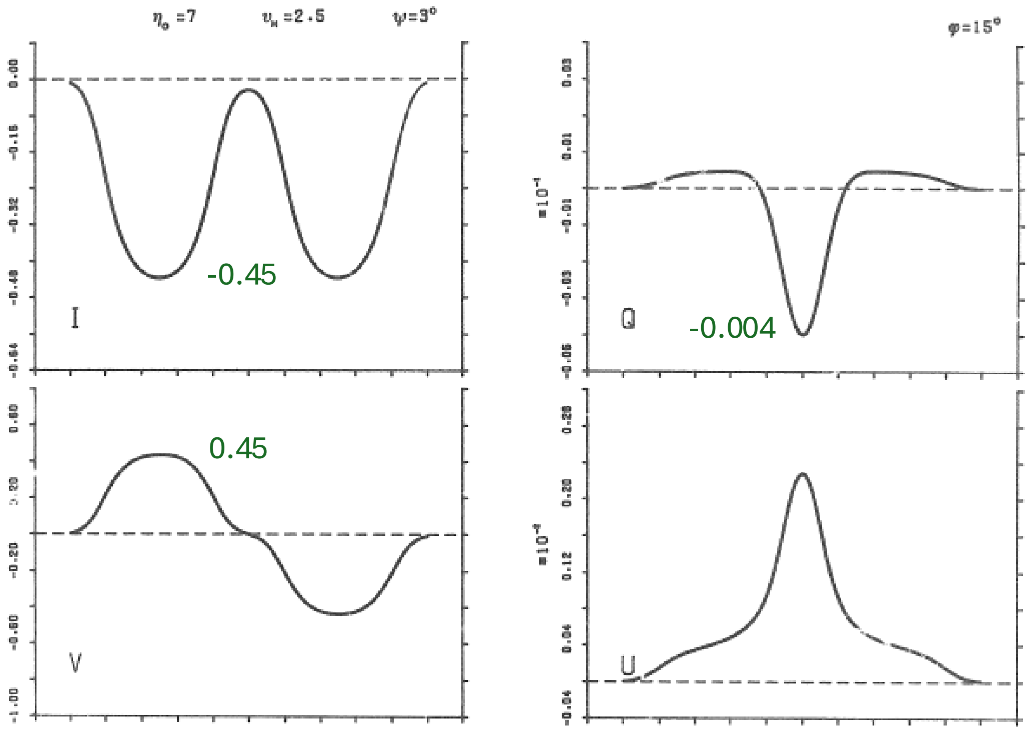

Nearly transverse $\vec{B}$

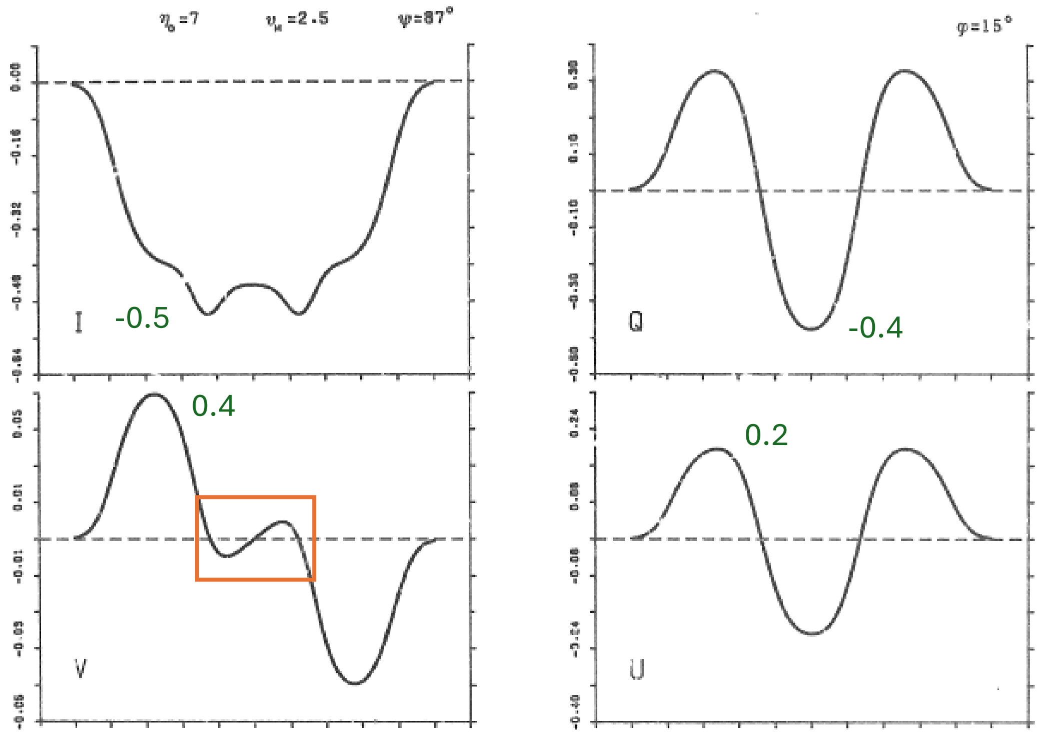

Magneto-optical effect

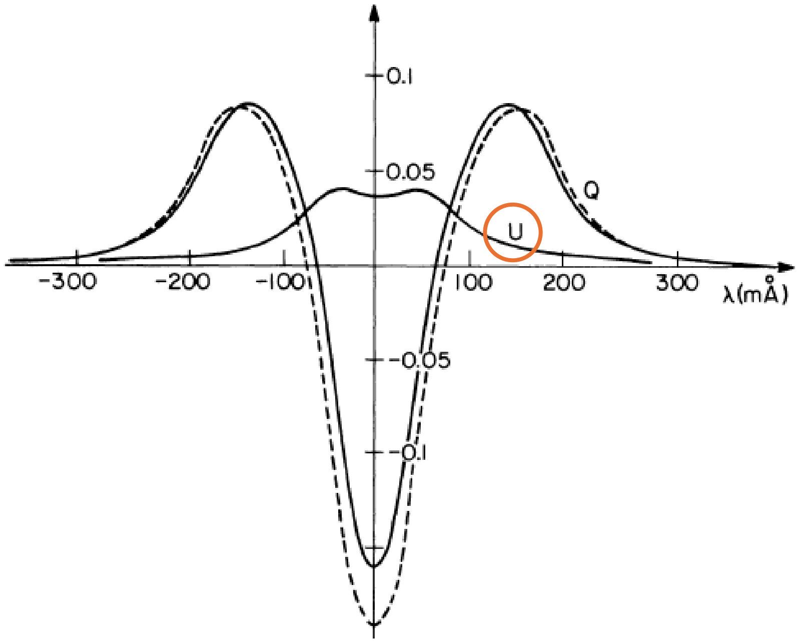

Fig. 1. Theoretical profiles of linear polarization Stokes parameters, expressed in units of the adjacent continuum, plotted as a function of wavelength for the Fe I λ5250 line. The dashed profile is the Q profile obtained neglecting magneto-optical effects. The profiles are computed using a numerical code described in Landi Degl'Innocenti (1976). The model sunspot atmosphere is from Henoux (1969) with a magnetic field of 3000 G inclined at 50° to the line of sight. The positive Q axis is assumed to be parallel to the magnetic field.

Landi Degl'Innocenti, SoPh, 63, 237-245 (1979), doi:10.1007/BF00174529

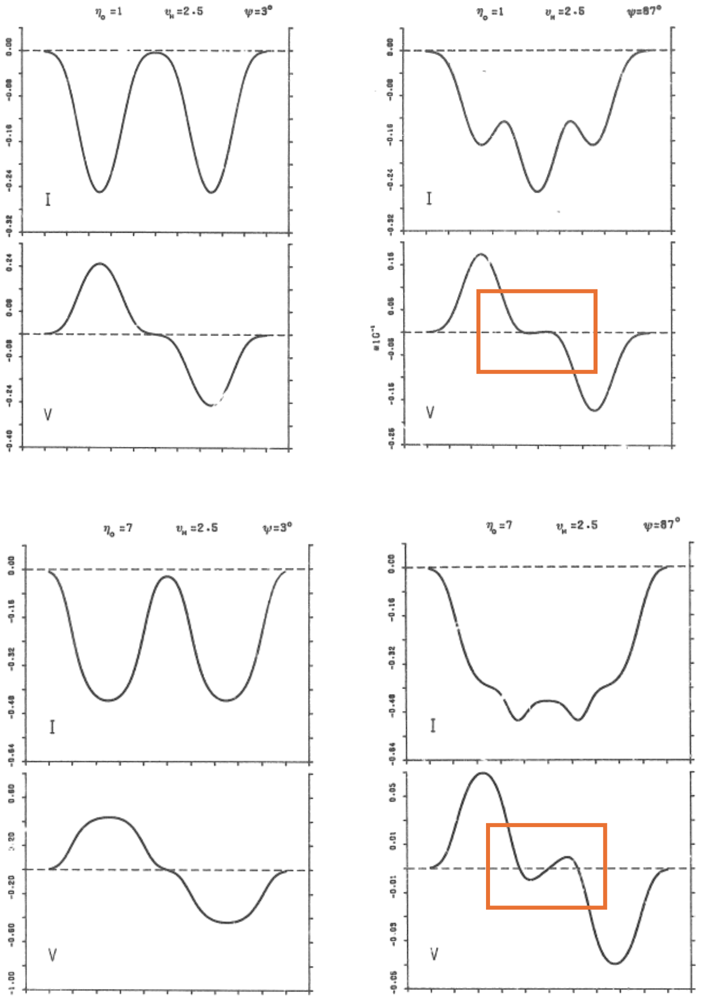

Weak line, strong splitting

Strong line, strong splitting

"Weak Zeeman splitting"

- In the astrophysical literature, "weak splitting" usually refers to the case $v_H \equiv v_b \ll v_D$.
- The simplified equations are often useful for a preliminary visualization of the behavior of the Stokes profiles. Magneto-optical effects are not included. The Voigt profile $H(a, v)$, where a is the damping parameter, may often be replaced by a simple Gaussian profile.

$$I(v) = B_0 + \frac{\mu B_1}{1 + \eta_0 H(a, v)} [1 + O(v_b^2)] ,$$

$$Q(v) = \frac{\mu B_1 H''(a, v)}{[(1 + \eta_0 H(a, v)]^2} \left(\frac{v_b \sin \gamma}{2}\right)^2 \eta_0[1 + O(v_b^2)] \cos 2\chi ,$$

$$U(v) = \frac{\mu B_1 H''(a, v)}{[1 + \eta_0 H(a, v)]^2} \left(\frac{v_b \sin \gamma}{2}\right)^2 \times \eta_0[1 + O(v_b^2)] \sin 2\chi + O(v_b^3) , \quad (50)$$

$$V(v) = \frac{-\mu B_1 H'(a, v)}{[1 + \eta_0 H(a, v)]^2} v_b \cos \gamma \, \eta_0[1 + O(v_b^2)] .$$

In our notation, $\gamma \to \psi$ and $\chi \to \phi$.

Jefferies+, ApJ, 343, 920 (1989), doi:10.1086/167762

“Weak Zeeman splitting”

$a = 0$ $v_b = 0.2$ B0 = 0 B1 = 1 $\mu = 1$ $\eta_0 = 1$ $\psi = 134°$ $\phi = 54°$

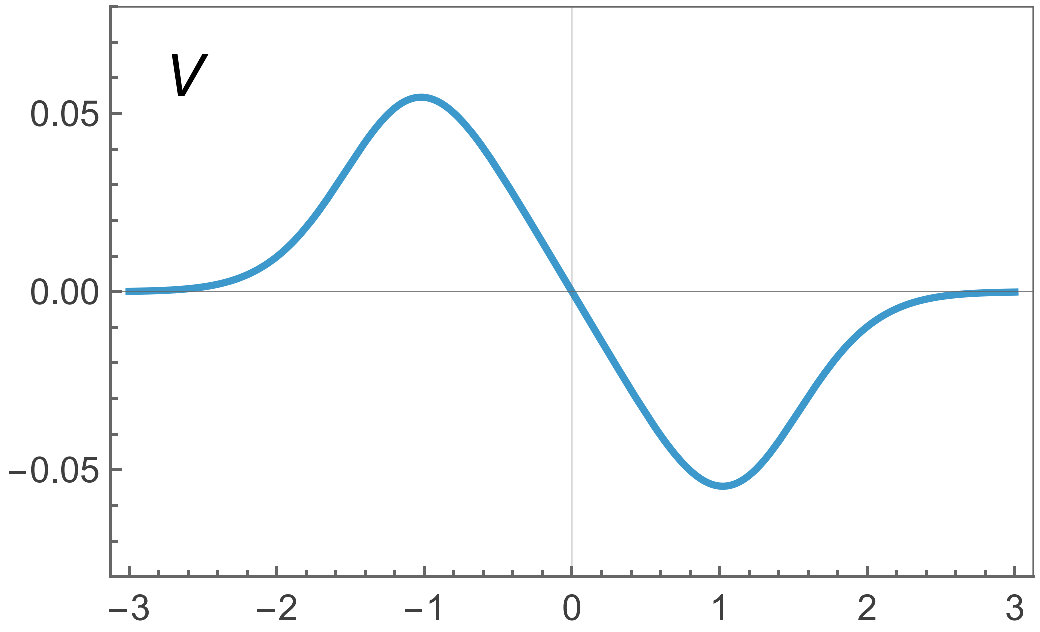

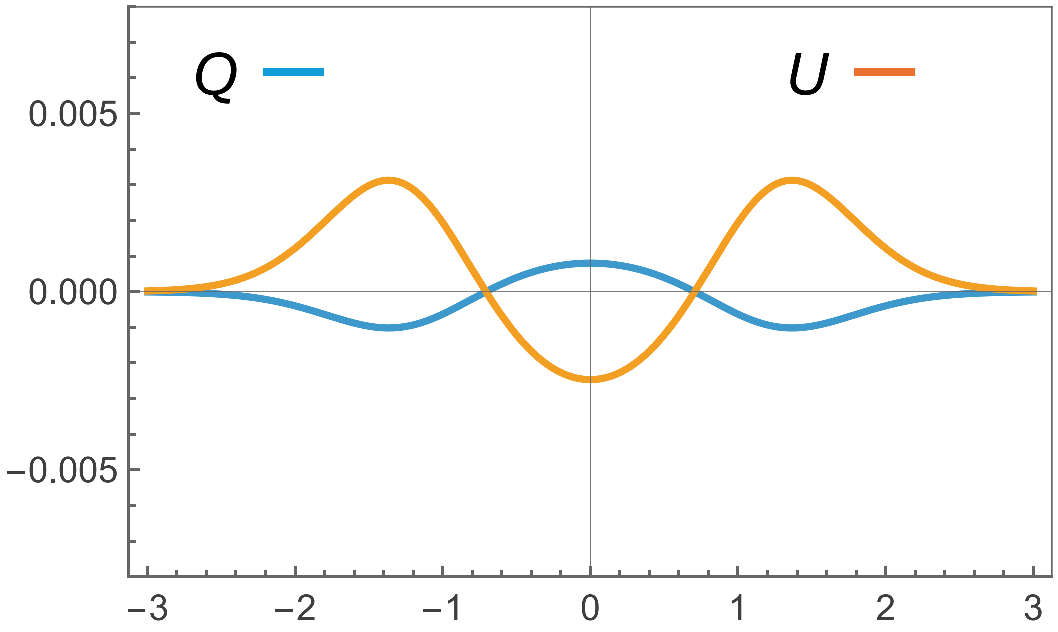

Pause for animation ...

Stokes profiles as a diagnostic tool

So, are we ready to roll? … *"If only life were fair."*

Ingredients of contemporary Stokes analysis

- Stuff from Landi Degl'Innocenti & Landolfi and later
- Model atmosphere
  - Preferably extracted from a radiative magnetohydrodynamic (MHD) simulation, including chromosphere and corona if needed
- Radiative transfer code
  - Non-LTE and must handle polarized radiation
  - Ideally 3D and including partial frequency redistribution (PRD) in scattering
- Observations! Modulation schemes (a lecture on its own)
- Stokes inversion code to infer $\vec{B}$ from $\{I,Q,U,V\}$ (another lecture) See, e.g., Jarolim+, ApJ, 985, L7 (2025), doi:10.3847/2041-8213/add342
- Parity disambiguation code for magnetograms

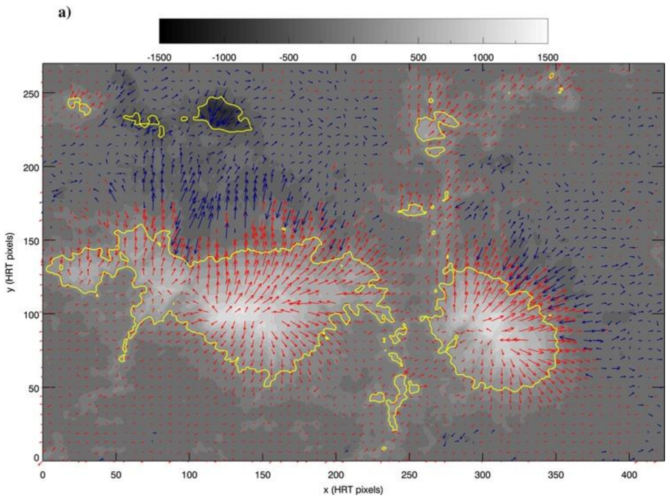

Valori+, A&A, 677, A25 (2023), doi:10.1051/0004-6361/202345859

Stokes in action – 1a

Schad+ 2024, Sci. Adv. 10, eadq1604, doi:10.1126/sciadv.adq1604

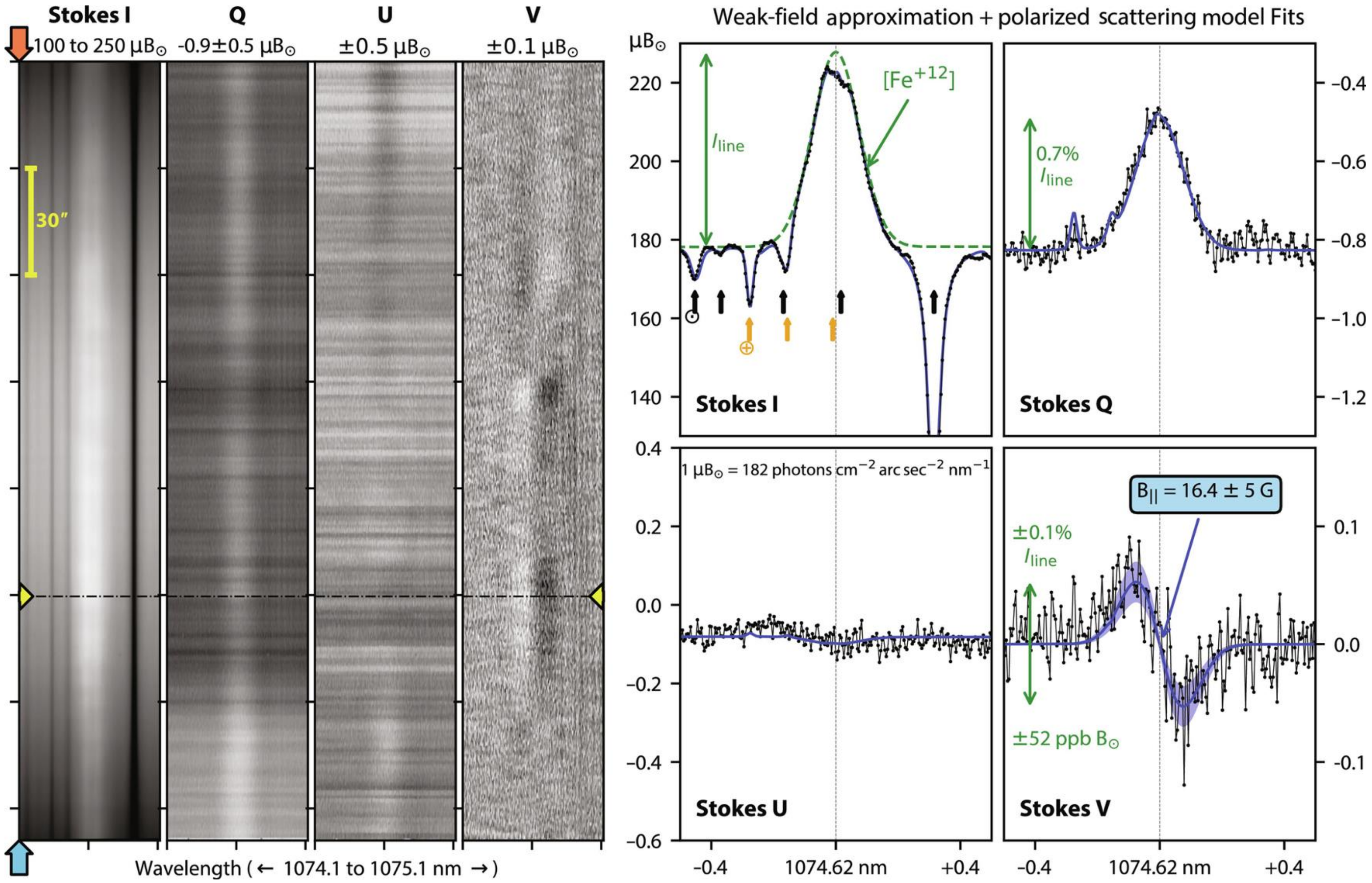

Fig. 2. DKIST/CryoNIRSP Fe^{+12} Stokes spectra and model fitted profiles. Left-hand images show the slit Stokes spectra of Fe^{+12} 1074 nm obtained near the lower portion of map A, as indicated by the blue and orange arrows in Fig. 1C. Each panel shows only a portion of the total observed spectral window. The antisymmetric signals in Stokes V, which show a polarity flip along the slit, are the first DKIST detections of the coronal Zeeman effect. A single Stokes profile extracted along the dashed line, corresponding to the location marked with a yellow arrow in Fig. 1, is plotted in the right-hand panels together with modeled profile fits. The locations of scattered photospheric lines in Stokes I are identified with black arrows, while orange arrows indicate terrestrial absorption lines. Here, the reference direction for Stokes +Q is tangential to the slit axis and therefore, to a fair approximation, radial with respect to the Sun.

Stokes in action – 1b

Schad+ 2024, Sci. Adv. 10, eadq1604, doi:10.1126/sciadv.adq1604

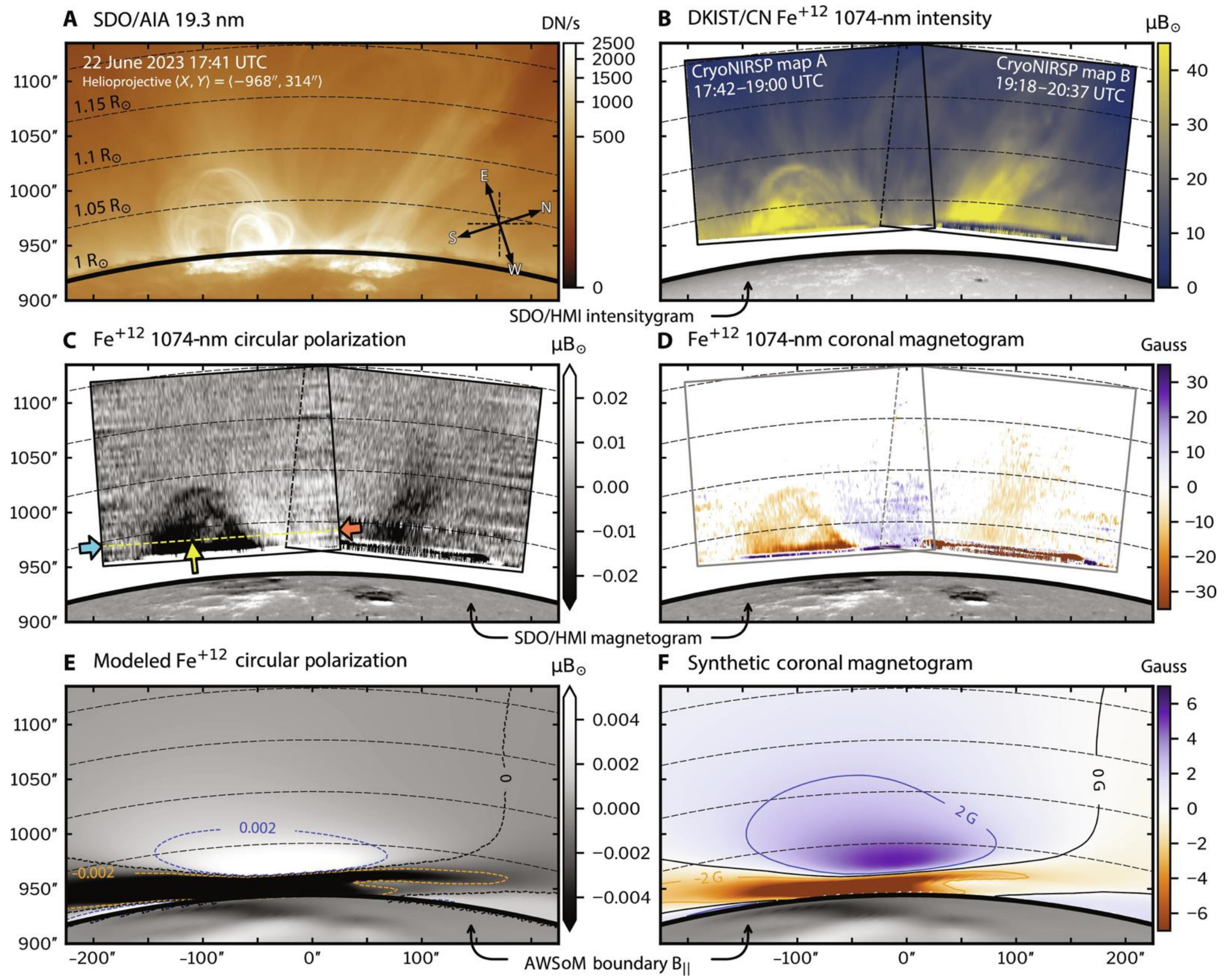

Fig. 1. The first DKIST coronal magnetogram mapping the magnetic field intensity.
(**A**) SDO/AIA 19.3-nm image cropped and rotated to geometry of DKIST/CryoNIRSP observations. Vertical coordinates give arc seconds from the center of the solar disk.
(**B**) The peak line amplitude of Fe^{+12} 1074 nm observed within the overlapping raster maps of CryoNIRSP in units of parts per million of the solar disk intensity, i.e., $\mu B_{\odot}$.
(**C**) Peak red-wing amplitude of the measured antisymmetric circular polarized Fe^{+12} profile. (**D**) Inferred coronal longitudinal magnetogram in units of gauss as inferred from the weak-field approximation fitted to the circular polarized profiles. (**E**) Synthetic Fe^{+12} 1074-nm circularly polarized amplitude calculated from the Alfvén Wave Solar Atmosphere Model (AWSoM) coronal model. (**F**) Synthetic coronal magnetogram inferred from the signal in (E) in the same manner as (D).

Stokes in action – 2

Ishikawa+ 2023, *ApJ,* 945,125, doi:10.3847/1538-4357/acb64e

“Evidence for the Operation of the Hanle and Magneto-optical Effects in the Scattering Polarization Signals Observed by CLASP2 across the Mg II h and k Lines”

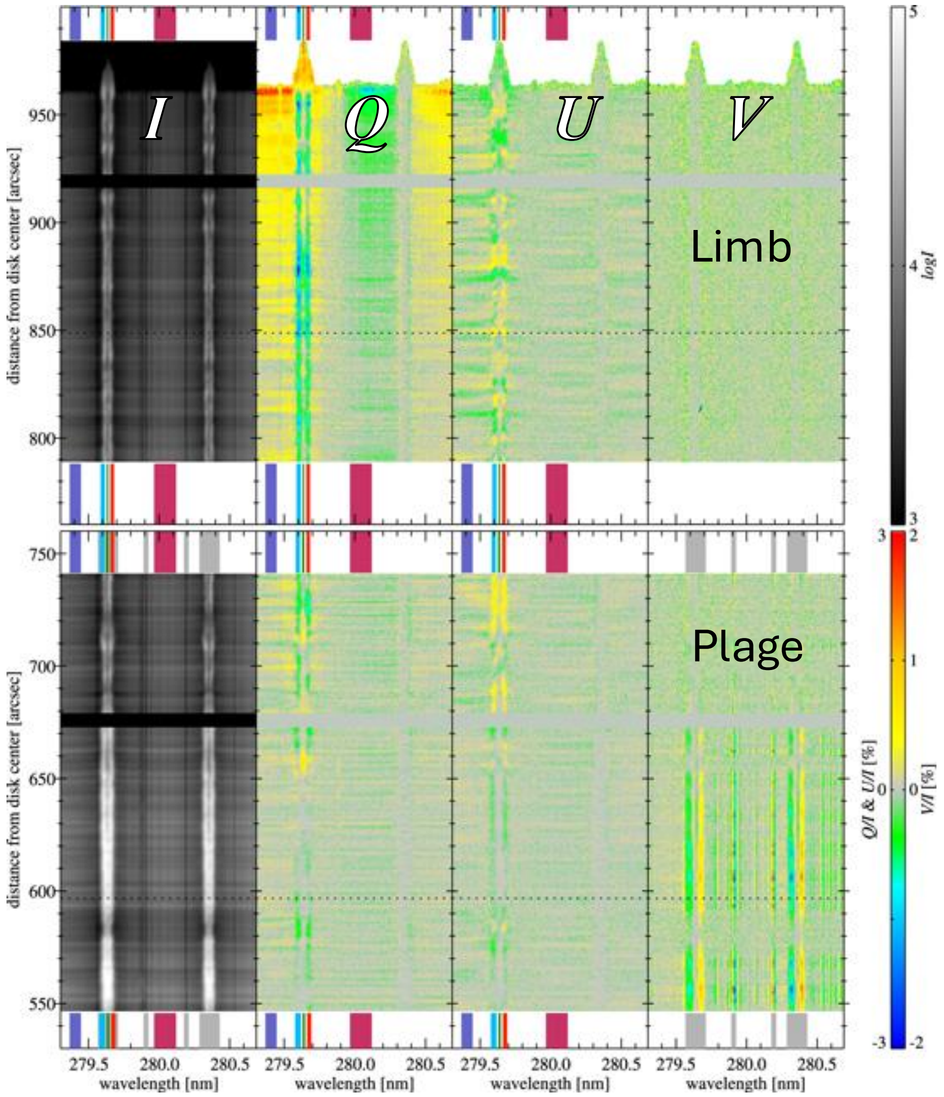

Figure 3. From left to right, temporally averaged intensity *I* and fractional polarization *Q/I*, *U/I*, and *V/I* spectra across the Mg ii h and k lines obtained by CLASP2 at the limb and plage targets (upper and lower panels, respectively). The intensity *I* is the averaged number of electrons per exposure detected by the two channels in logarithmic scale. The data under the dust on the slit, which are shown in black (in *I*) and gray (in *Q/I*, *U/I*, and *V/I*) horizontal stripes are excluded in the analysis. The Stokes signals corresponding to each of the spectral ranges colored with violet, light blue, green, red, and magenta have been integrated for obtaining the far blue wing, the near blue wing, the core, the near red wing, and the far red wing signals explained in the text. The colors are the same as those in Figures 4 and 5. The gray areas in the *I* and *V/I* panels indicate the spectral regions of the Mg ii k (279.64 nm), Mn II blue (279.91 nm), Mn II red (280.19 nm), and Mg II *h* (280.35 nm) lines, respectively, across which we have applied the WFA to estimate the longitudinal component of the magnetic field at different heights in the solar atmosphere.

Magnetograms

- A magnetogram is a data cube of the magnetic field (1, 2, or 3 components) in 2 or 3 spatial dimensions, and possibly time.
- A magnetogram can be formed by scanning the slit of a spectrographic polarimeter across a region of the Sun.
  - This is generally a slow process.
  - Faster approaches include multiple slits, an integral field spectrograph, or an energy-resolving detector.
- More commonly, narrowband filters or interferometers are used to sample 2 or more wavelengths in the profile of a magnetically sensitive line (see figure), obtaining Stokes data for each position.
- A filter magnetograph should be calibrated against high-resolution Stokes profiles, real or simulated.

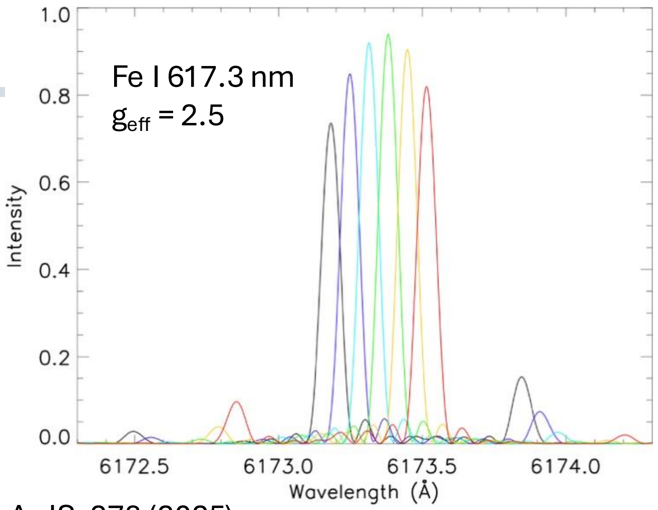

Petrie+, ApJS, 278 (2025), doi:10.3847/1538-4365/adcf9f

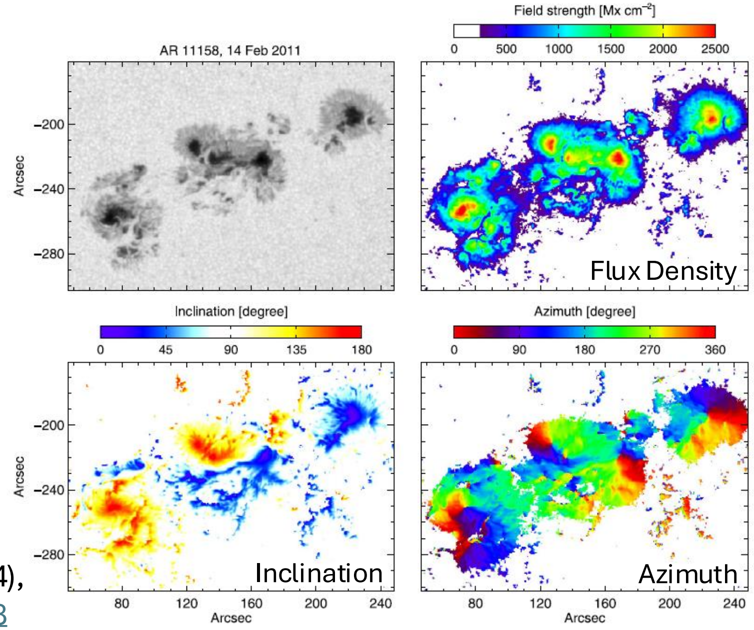

Hoeksema+, SolPhys, 289 (2014), doi:10.1007/s11207-014-0516-8

Magnetograms—the Large

- Full-disk magnetograms are particularly important because of their many applications.
  - Measurements of magnetic flux for studying and forecasting the solar activity cycle
  - Setting boundary conditions for extrapolating the magnetic field into the corona
  - Identifying magnetic regions with more than average likelihood to be associated with energetic events such as mass ejection or flares (applications to space weather)
- The evolution of the polar magnetic field is key to solar cycle studies, but it is difficult to study from Earth because the Stokes V signal is very weak on average → Solar Orbiter and future missions.
- A small error in the zero-point of a magnetic flux map can have a significant effect on magnetic field extrapolations and flux transport studies → calibrations and recalibrations.
- Magnetic synoptic maps (right) are another important derived product of full-disk magnetograms.

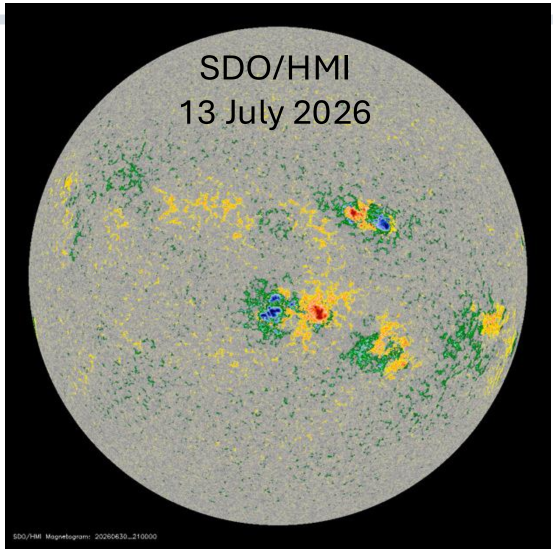

Carrington Rotation: 2313_186 14 Jul 2026 22:14 UT

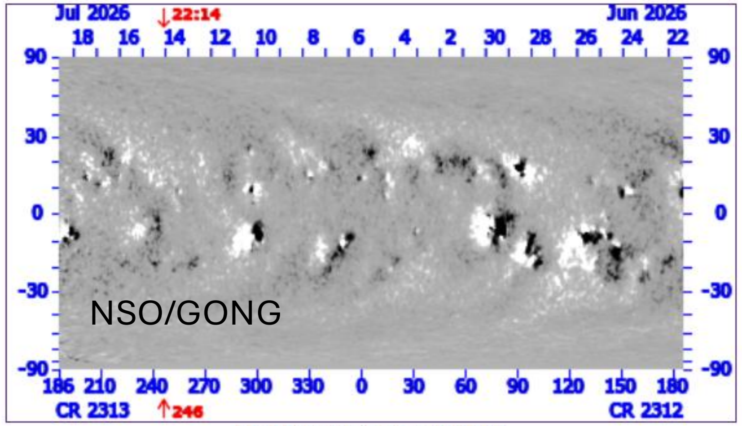

Magnetogram Count: 7043

Magnetograms—the Small

- The smallest resolvable magnetic field concentrations are fascinating and a vital connection to theory and MHD simulations of the solar atmosphere.
- Magnetic flux measurements that include unresolved concentrations of opposite polarity can affect derived quantities such as the amount of open solar magnetic flux.

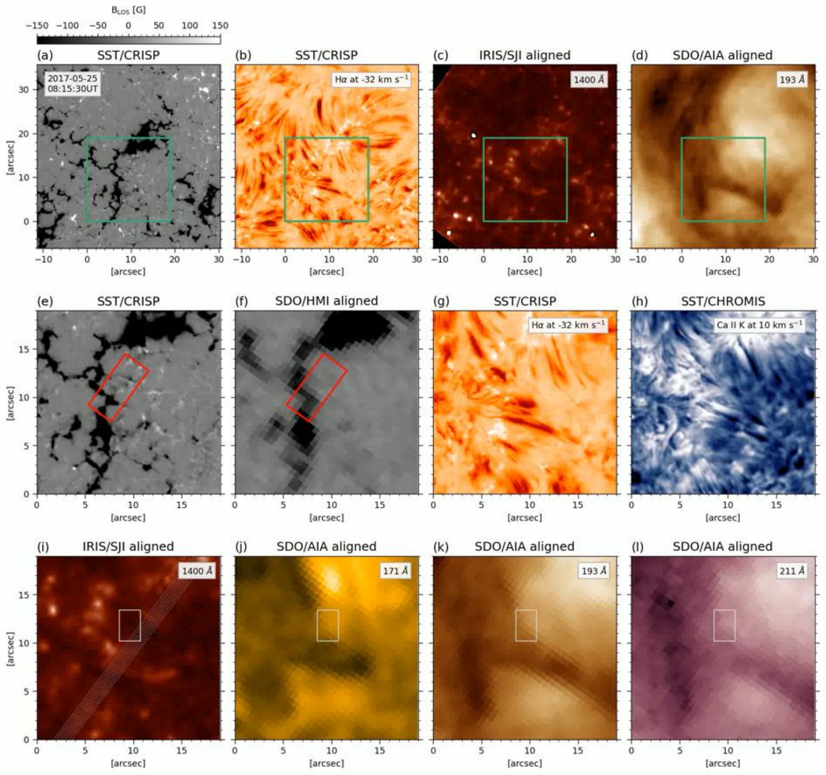

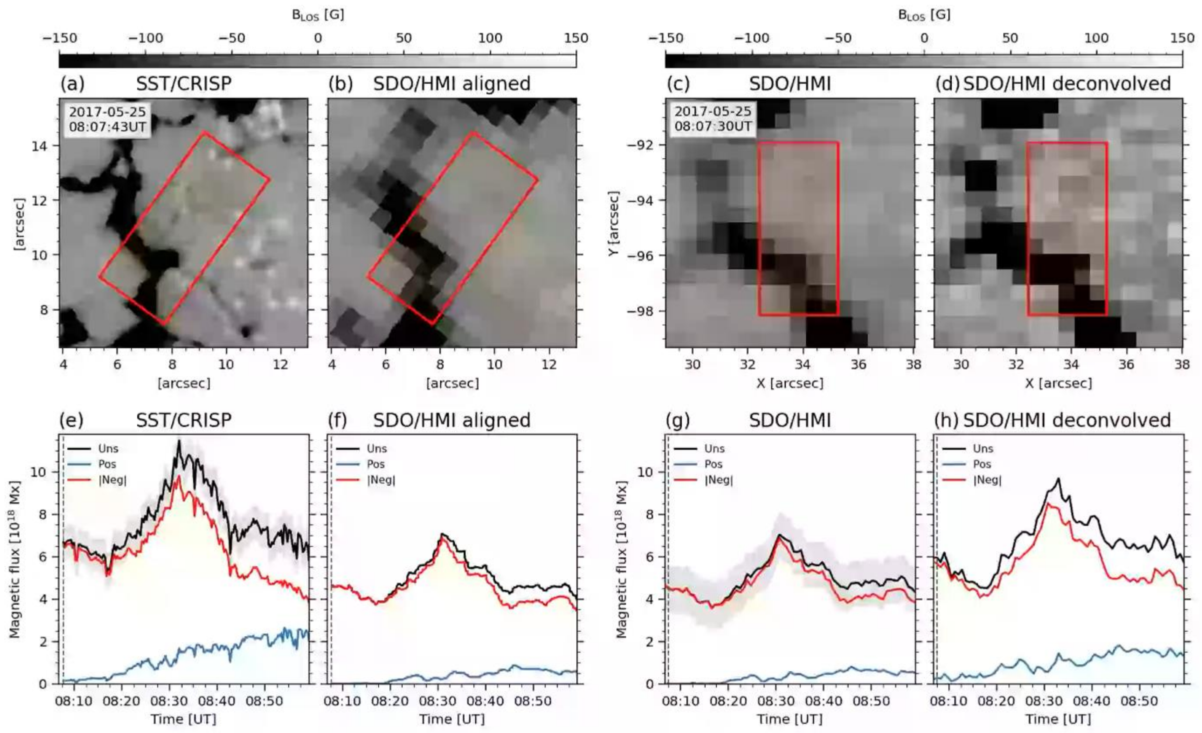

Nobrega-Siverio+, A&A, 686, A218 (2024), doi:0.1051/0004-6361/202348894

Polarization everywhere

Take-aways

- Scattered light may be polarized when the incident radiation field is anisotropic.
- Global anisotropy is common for observations near the solar limb. Local anisotropy is guaranteed at some level because the solar atmosphere is horizontally inhomogeneous.
- Solar limb darkening prevails in the visible spectrum which, for dipole-type scattering, causes linear polarization oriented parallel to the limb.
- Ubiquitous linear polarization in the solar spectrum caused by coherent scattering processes has been called the "Second Solar Spectrum". *

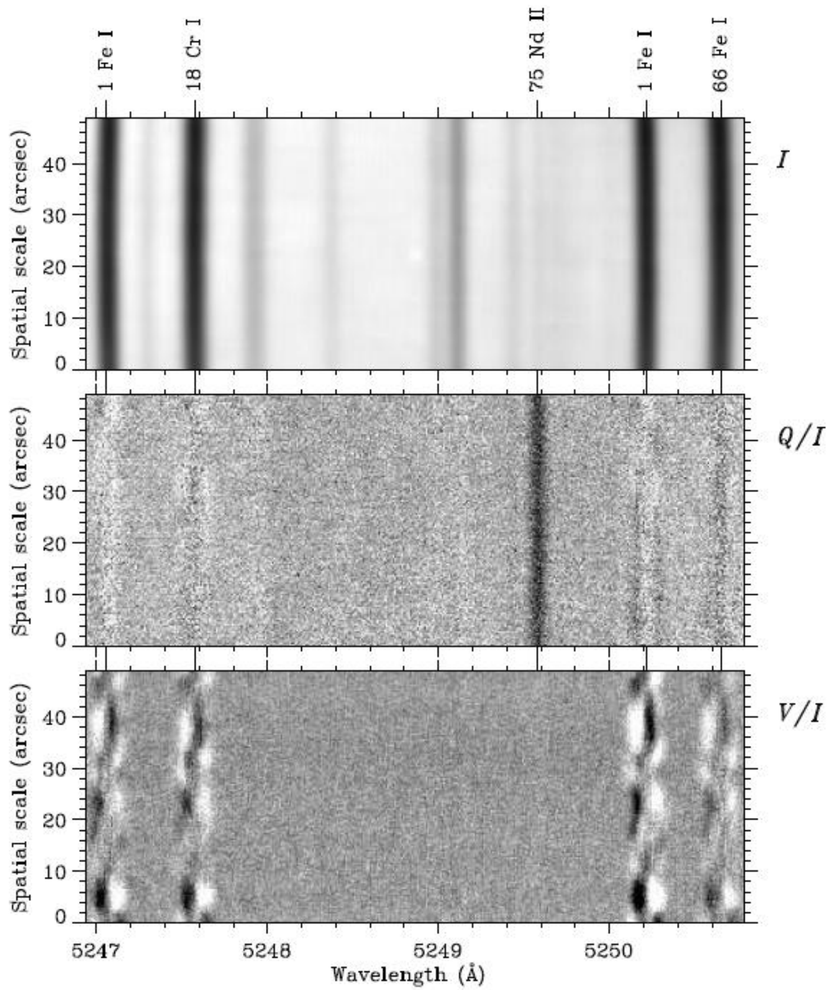

Spectrum obtained 5 arcsec inside the solar limb (μ=0.1) with the ZIMPOL imaging Stokes polarimeter.*

* Stenflo & Keller, A&A, 321, 927-934 (1997)

Photospheric continuum polarization

- We discussed scattering polarization in connection with the Hanle effect on spectral lines in a magnetic field.
- The photospheric continuous spectrum is also weakly (< 1%) linearly polarized by coherent scattering. The main sources are Rayleigh scattering from neutral hydrogen and Thomson scattering from free electrons.
- Thomson scattering is elastic scattering of an electromagnetic wave by a free charged particle.
  - The wave exerts a Lorentz force on the particle, which oscillates at the same frequency and emits dipole radiation at that frequency.
  - If the photon energy approaches the rest-mass energy of the particle (511 keV for electrons), different kinematics apply (Compton scattering).
- There are two monochromatic emission coefficients j_ν (power scattered by dV and dν into dΩ) associated with Thomson scattering, one for radially polarized light and one for tangentially polarized light. For unpolarized incident light,

$$j_{\text{tan}} = nF_\nu \frac{3}{16\pi}\sigma_T \qquad j_{\text{rad}} = nF_\nu \frac{3}{16\pi}\sigma_T \cos^2\chi \quad \text{where n is the density}$$

of scattering particles of charge q, F_ν is incident flux, and $\sigma_T = \frac{8\pi}{3}\left(\frac{q^2}{4\pi\varepsilon_0 mc^2}\right)^2$

- Note: (1) Radial emissivity has a classic dipole pattern.
  (2) σ_T is independent of wavelength.

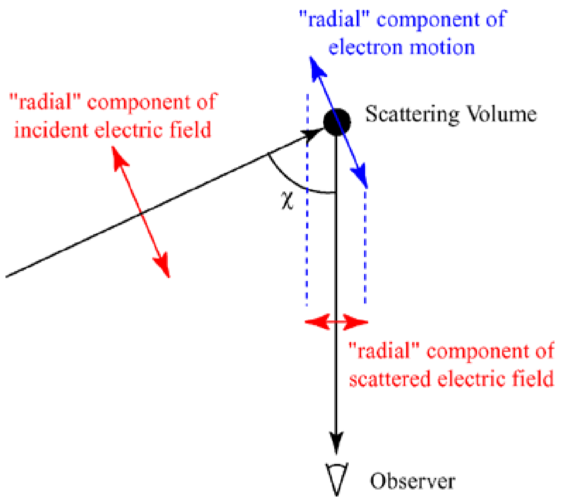

Thomson scattering. The "radial" component of $\vec{E}$ is in the plane of the diagram. "The tangential" component (perpendicular to plane) is unaffected. Graphic by PAR via Wikimedia.

Photospheric continuum polarization

- In Rayleigh scattering from an atom or molecule (bound system), the incident electric field induces an oscillating dipole moment in the particle, which then radiates.
- Rayleigh scattering scattering can be modeled classically by the Lorentz "damped spring" model of a bound electron. In the solar photosphere, the cross section for Rayleigh scattering from neutral hydrogen is strongly wavelength dependent, $\sigma_R/\sigma_T \approx (\nu/\nu_0)^4$ where ν_0 is the resonant frequency of the oscillator in the Lorentz model.
- Numerically, for $\lambda > 200$ nm, $\sigma_R/\sigma_T \approx (96.6/\lambda)^4\,[1 + (156.6/\lambda)^2 + (148.0/\lambda)^4]$

Take-away

- Although the photospheric continuum polarization is small, it is not negligible, both as an independent diagnostic and as the background polarization upon which line-related polarization is superposed.

Photospheric continuum polarization

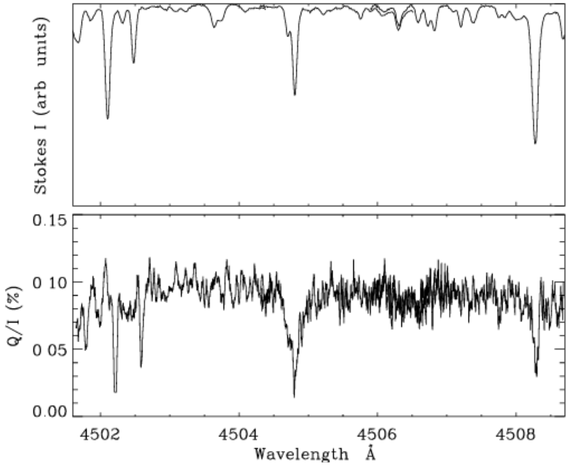

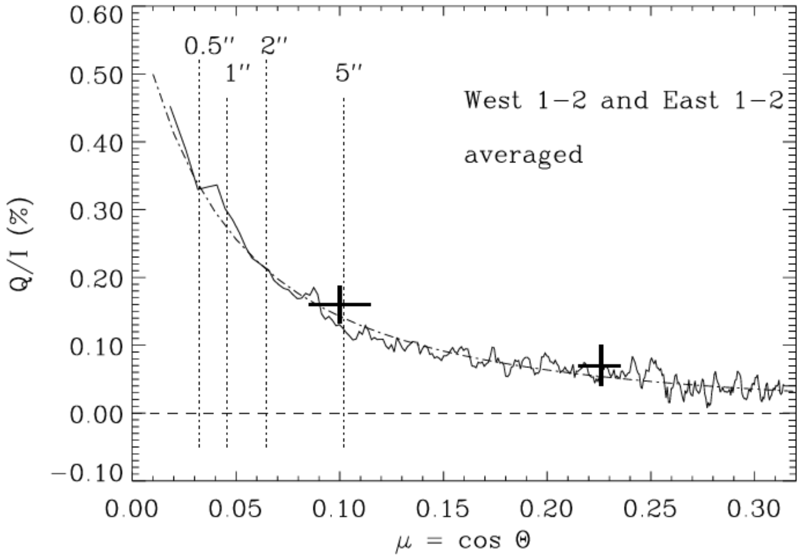

* Wiehr & Bianda, A&A, 398, 739-742(2003), [doi:10.1051/0004-6361:20021515](https://doi.org/10.1051/0004-6361:20021515)

Q/I vs λ at μ = 0.1

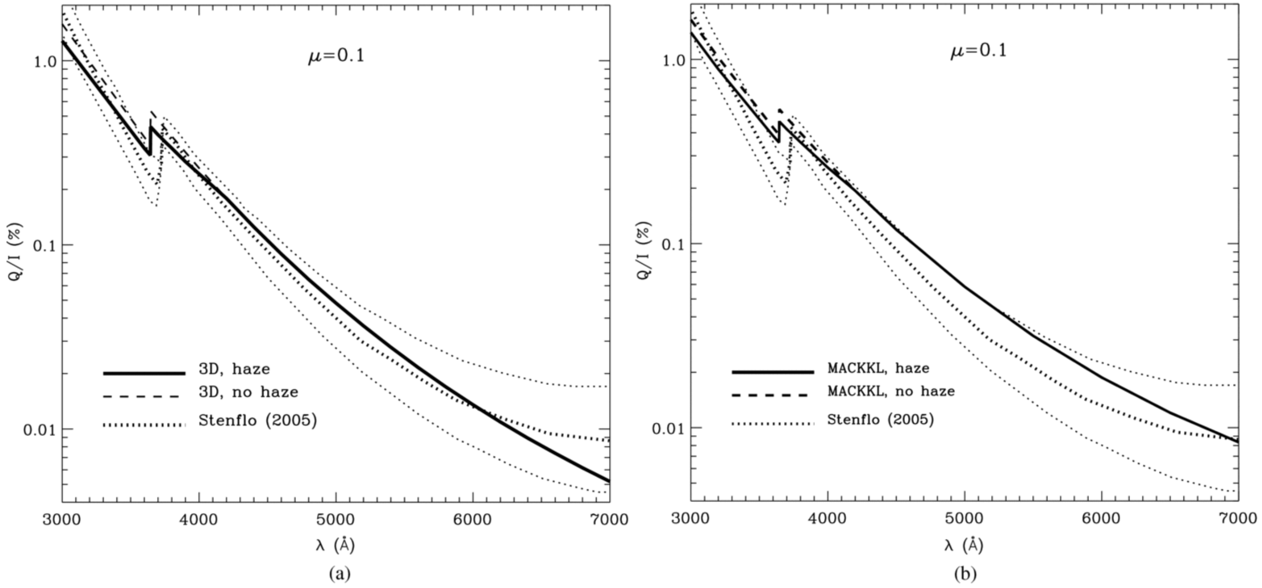

* Trujillo Bueno & Shchukina, A&A, 694 (2009), [doi:10.1088/0004-637X/694/2/1364](https://doi.org/10.1088/0004-637X/694/2/1364)

* Stenflo & Keller, A&A, 321, 927-934 (1997)

Differential Emission Measure

Take-aways

- The differential emission measure (DEM) is a powerful tool for assessing the distribution of temperatures along the line of sight in coronal plasma.
- The DEM is undefined for an optically thick plasma.

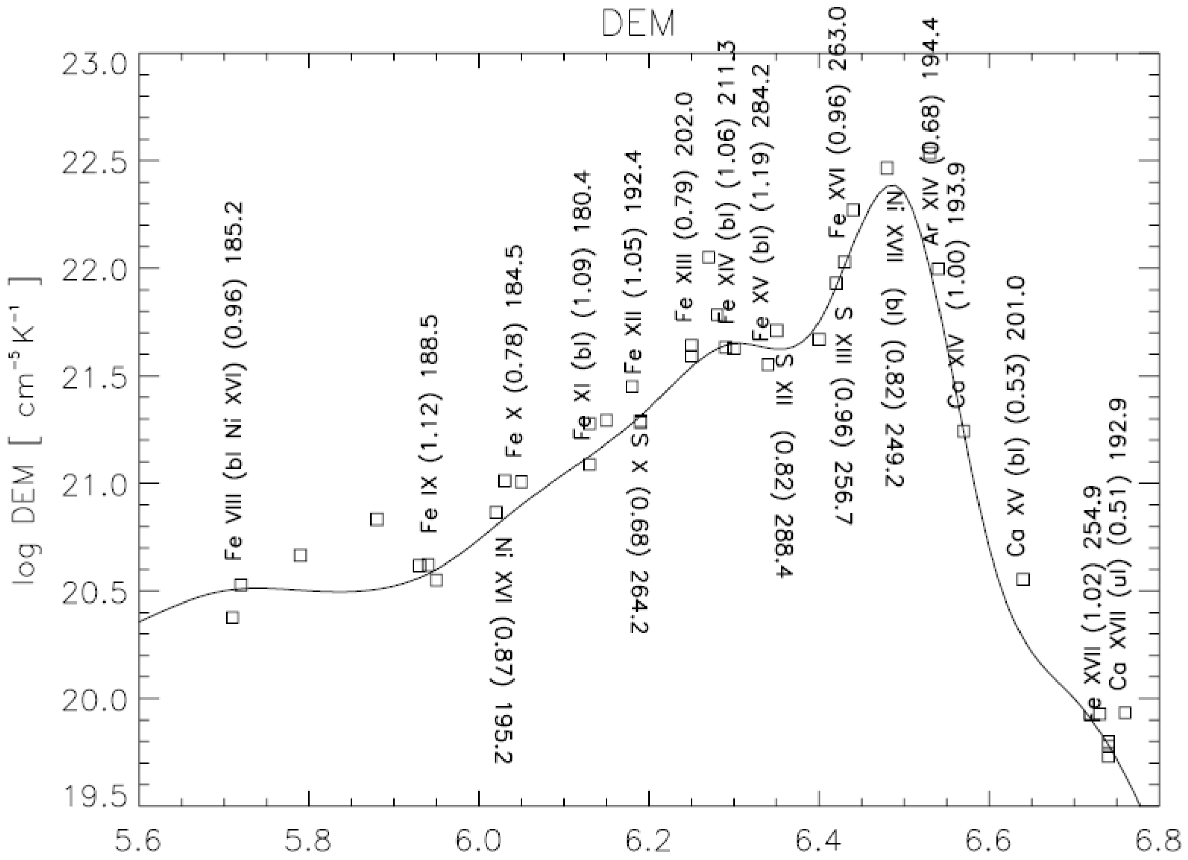

Del Zanna, A&A, 558 (2013), A73, doi:10.1051/0004-6361/201321653

Differential Emission Measure $\phi(T)$

Assumptions

- Excitation of both line and continuum emission is due to collisions of free electrons with protons and heavier ions.
- The plasma is optically thin.

Definition*

$$\phi(T) = N_e N_h \frac{dh}{dT} \quad [\mathrm{m^{-5}K^{-1}}]$$

where h is the column depth attributed to temperature T

- The *radiance* of a line is $I = \epsilon \int_h N_e N_h\, G(T, N_e)\mathrm{d}h$ or $I = \epsilon \int_h G(T, N_e)\phi(T)\mathrm{d}T$

  where ϵ is the abundance of the emitting element relative to hydrogen, and N_h is the number density of hydrogen (protons + neutrals).
- The contribution function G is defined as $G(T, N_e) = \frac{1}{2N_e} \hbar\nu\, n_j(T, N_e)F(T)A_{ji}$ where n_j is the population of the emitting level relative to the total population of the ion, F is the ionization fraction of the emitting ion, and A_{ji} is the radiative decay rate for the transition.

* We adopt definitions and notation from Chianti. Small variants are found in the literature.

Contribution functions

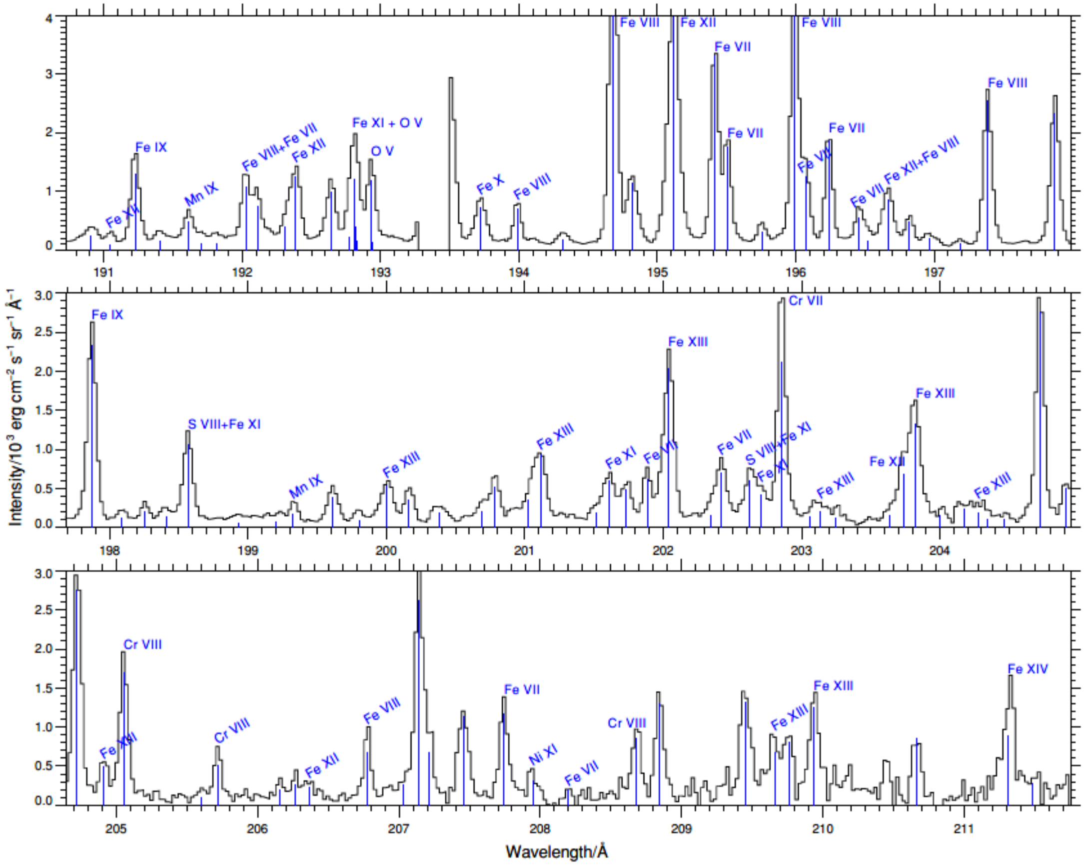

Spectrum from Hinode/EIS

Landi & Young, A&A 539, A146 (2012), doi:10.1088/0004-637X/706/1/1

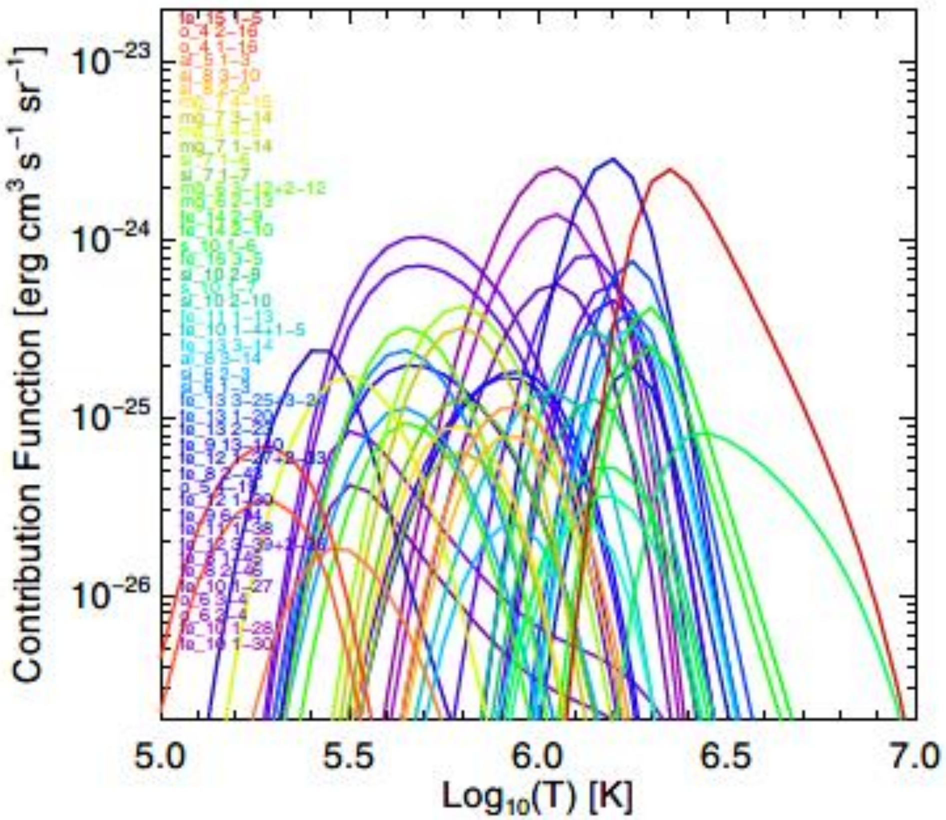

Computed contribution functions for selected EIS lines

Hannah & Kontar, A&A 539, A146 (2012), doi:10.1051/0004-6361/201117576)

Differential Emission Measure

- You can now interpret a DEM constructed from observations of individual spectral lines (2 slides back).
- In the case of a passband instrument such as SDO/AIA, the contribution function is replaced by the instrument response, which is calculated by summing all the $G(T, N_e)$ of the lines in the passband, accounting for telescope effective area as a function of wavelength within a passband and adding the emissivity of the continuum.

Filter	Ions	Log T
131	Fe VIII, XX, XXIII	5.6, 7.0, 7.2
171	Fe IX	5.8
193	Fe XII, XXIV	6.1, 7.3
211	Fe XIV	6.3
335	Fe XVI	6.4
94	Fe XVIII	6.8

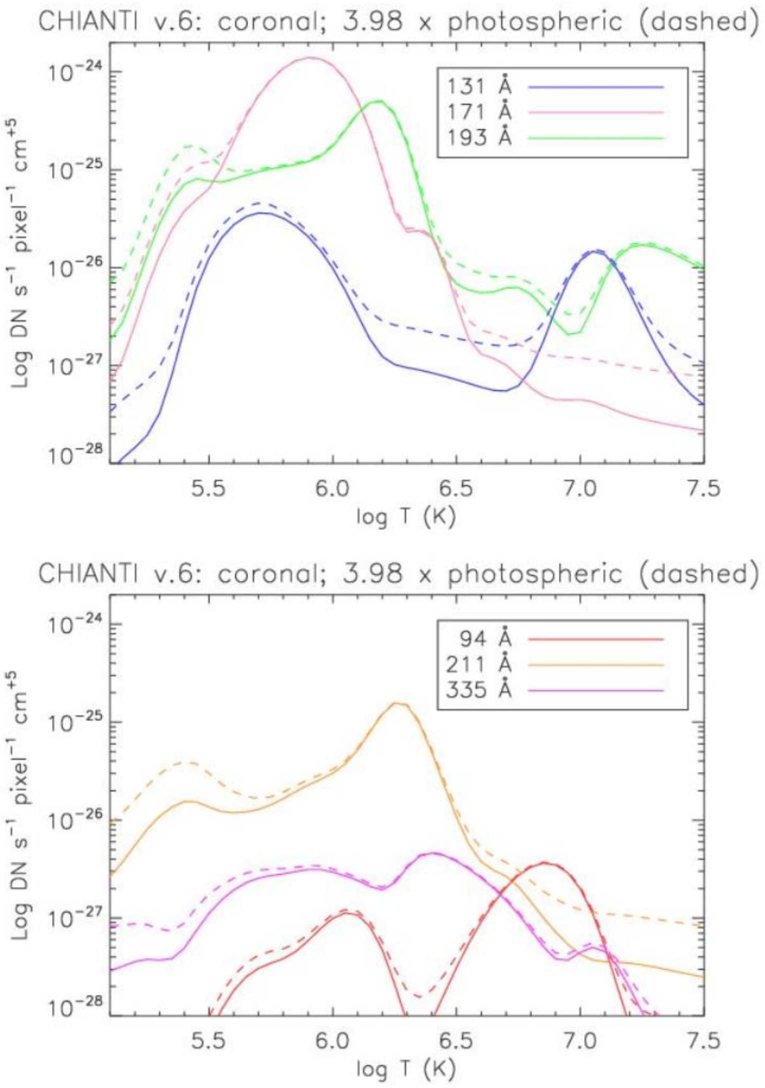

Del Zanna+, A&A, 535, A46 (2011)
doi:10.1051/0004-6361/201117470
(use the latest curves from Solarsoft!)

Differential Emission Measure

Ahem …

- … we've conveniently skipped over something.
- Whether we use spectroscopic or passband observations, what we want, $\phi(T)$, is embedded in an integral equation,

$$I = \epsilon \int_h G(T, N_e)\phi(T)\mathrm{d}T$$

- Solving this equation for $\phi(T)$ has been known for many years to be an ill-posed inverse problem. A direct approach to a solution normally amplifies observational uncertainties and yields spurious results.
- Robustly recovering the DEM and its associated uncertainties is a well-established cottage industry. One still-useful approach to regularized inversion is given by Hannah & Kontar (top figure).
- Supervised machine learning has been applied to DEM inversion by Wright et al. (2019) (bottom figure).
- Further ML and AI approaches to both DEM inversion and Stokes inversion are developing rapidly. Examples: Youn+, A&A, 695, A125 (2025), doi:10.1051/0004-6361/202452304 and Campbell+, ApJ, 998 (2025), doi:10.3847/1538-4357/addb49

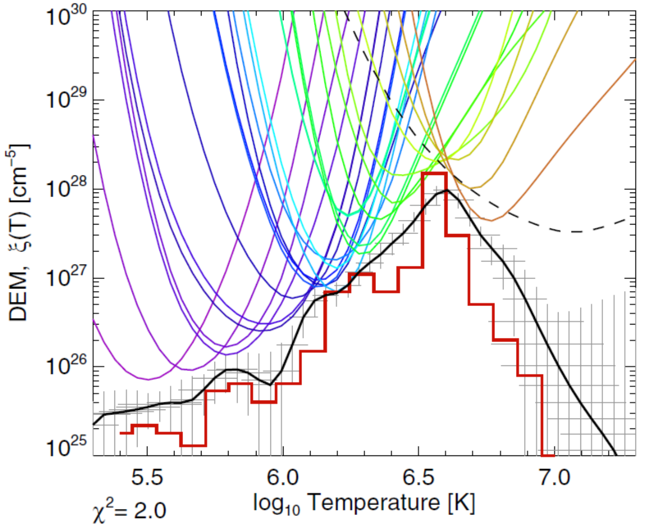

Hannah & Kontar, A&A 539, A146 (2012), doi:10.1051/0004-6361/201117576)

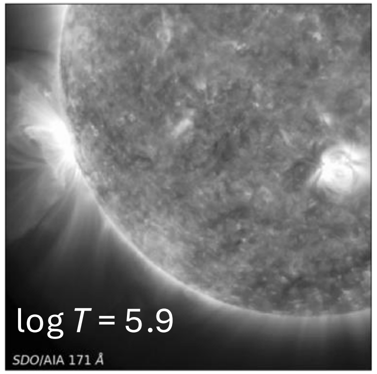

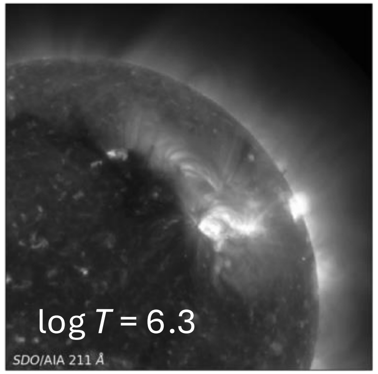

Wright+, zenodo.org (2019), doi:10.5281/zenodo.2587015

Differential Emission Measure

- Early in the development of the DEM diagnostic, the available data and theory were more suited to generic, "average" characterizations of the DEM – "quiet Sun", "active region", "bright point", etc.
- Today the emphasis is on DEM maps that reveal how the temperature distribution in the line of sight varies over a specific field of view.
- As there is a one-dimensional distribution of temperature at each spatial pixel, VR should be a useful tool for exploring the data cube.

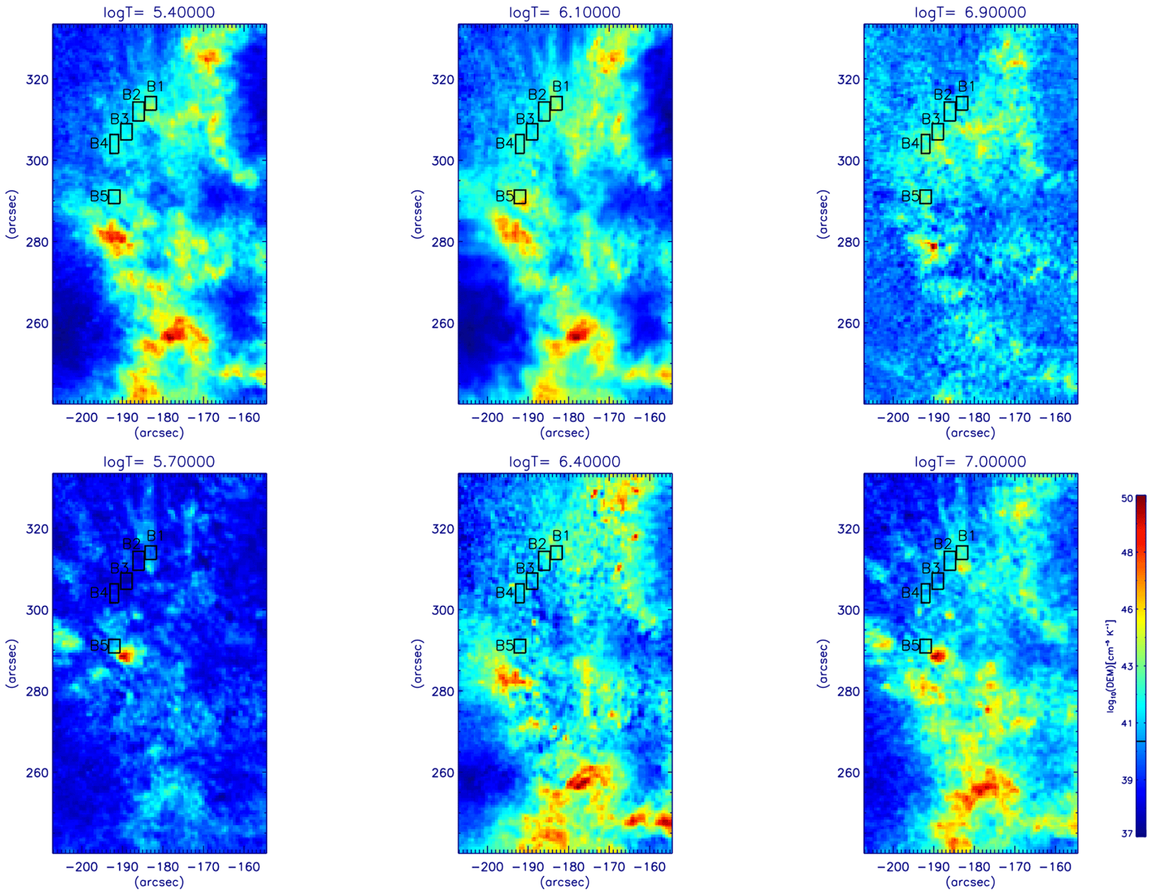

Rao+, Ann. Geophys., 37 (2019), doi:10.5194/angeo-37-765-2019

3D (Tomographic) DEM

- With multiple viewpoints, it is possible to overcome the line-of-sight confusion inherent in single-viewpoint observations of an optically thin medium.
- The tomographic process starts with voxelizing a computational domain spanning some range in height above the limb.
- Each voxel has its own volume emissivity, dependent on temperature, density, and abundances.
- The formalism for relating the contribution from a given voxel to the flux observed through a particular filter along a specific line of sight is conceptually the same as for the usual DEM (but geometry is tricky).
- The observations must then be inverted to obtain *local* DEMs, again conceptually like the standard DEM case but more challenging.

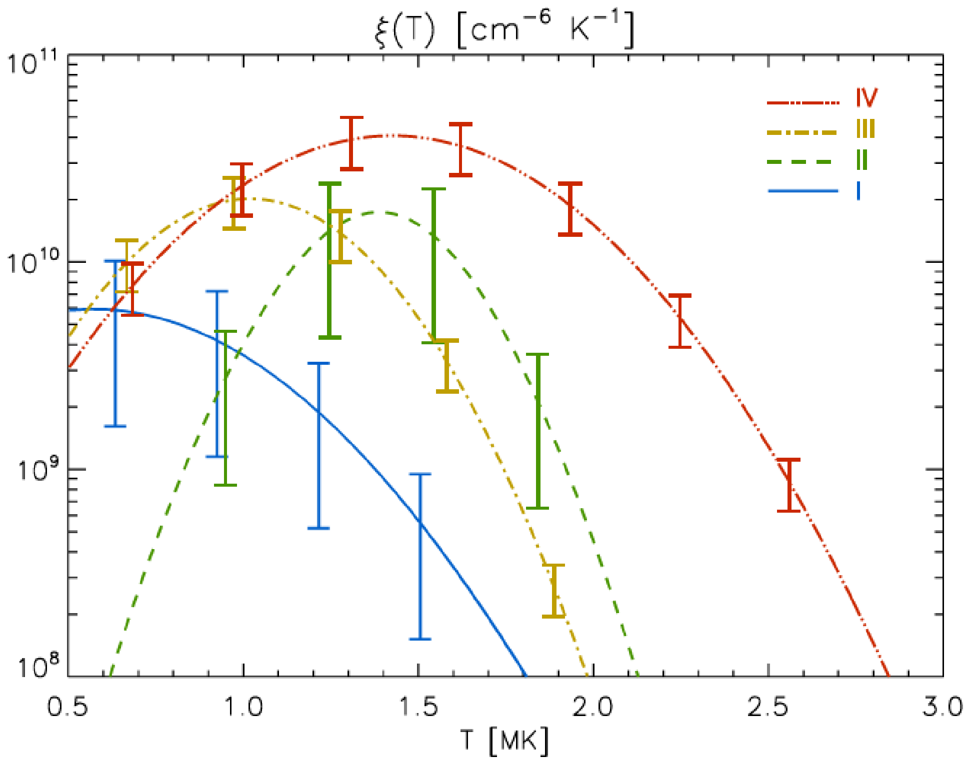

Figure 5. LDEM curves (assuming a Gaussian functional form) for regions I, II, III, and IV (at 1.075 R_S) in Figure 4. Regions I and II are subpolar "quiet Sun," of low and high density, respectively. Region III is equatorial "quiet Sun" and region IV is an AR.

See also Jarolim+, "3D Reconstructions of the Solar EUV Corona with Neural Radiance Fields", BAAS 57, e-id 2025n4i309p02 (2025)

Frazin, Vásquez & Kamalabadi, ApJ, 701, 1 (2009), doi:10.1088/0004-637X/701/1/547

Stokes modulation and demodulation

- A single state of a polarimeter can be characterized by a modulation vector $\mathbf{m}$ that prescribes the action of the polarimeter on an incident Stokes vector, $\boldsymbol{S} = \{S_1, S_1, S_1, S_1\} = \{I, Q, U, V\}$: $\mathcal{I}_{\text{out}} = \mathbf{m} \cdot \mathbf{S}_{\text{in}}$. For example, $\mathbf{m} = \{0,0,0,1\}$ extracts only Stokes *V*.
- An n-state polarimeter is characterized by a 4×n modulation matrix $\boldsymbol{M}$ such that the n exit fluxes $\boldsymbol{\mathcal{I}}_{\text{out}}$ of the polarimeter are given by $\boldsymbol{\mathcal{I}}_{\text{out}} = \boldsymbol{M}\,\mathbf{S}_{\text{in}}$. We need n ≥ 4 to measure 4 Stokes parameters.
- Demodulation is used to deduce the incident Stokes parameters from measured fluxes: $\mathbf{S}_{\text{in}} = \boldsymbol{M}^{-1}\,\boldsymbol{\mathcal{I}}_{\text{out}}$
- Real-world example: polarimeter comprising two Liquid Crystal Variable Retarders (LCVRs) and a linear polarizer (LP) with the arrangement shown in the figure. This configuration is used by the Polarimetric and Helioseismic Imager on Solar Orbiter (SO/PHI).

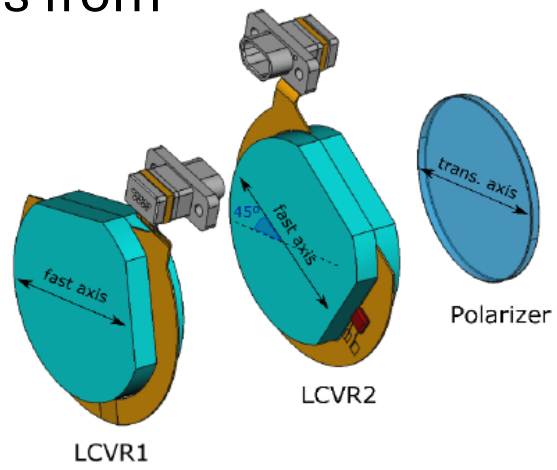

Stokes modulation and demodulation

- LCVR1 has 2 retardance states: 0°, 90°
- LCVR2 has 4 retardance states: 0°, 90°, 180°, 270°

LCVR1 retardance (°)	LCVR2 retardance (°)	Modulation Vector	Output
0	0	{1, +1, 0, 0}	I + Q
0	180	{1, -1, 0, 0}	I - Q
90	90	{1, 0, +1, 0}	I + U
90	270	{1, 0, -1, 0}	I – U
0	90	{1, 0, 0, +1}	I + V
0	270	{1, 0, 0, -1}	I – V

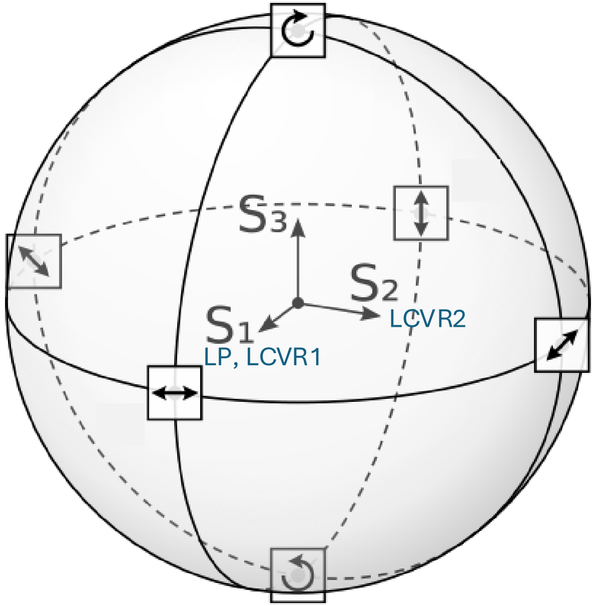

- With a polarizing beamsplitter in place of the LP, only 4 modulation states are required.
- It is not necessary to modulate for "pure" output states. More complex linear combinations of the Stokes parameters may be more efficient. The efficiency can be evaluated by examining the demodulation matrix $\boldsymbol{M}^{-1}$.*

* Del Toro Iniesta & Collados, ApOpt, 39 (2000), doi:10.1364/AO.39.001637
"Optimum modulation and demodulation matrices for Solar polarimetry"

Thanks again!